CAPACITY RELATED PROPERTIES AND ASSESSMENT OF SCHOOL BUILDINGS IN TURKEY

A THESIS SUBMITTED TO
THE GRADUATE SCHOOL OF NATURAL AND APPLIED SCIENCES
OF
MIDDLE EAST TECHNICAL UNIVERSITY

BY

İLKER KALEM

IN PARTIAL FULFILLMENT OF THE REQUIREMENTS
FOR
THE DEGREE OF MASTER OF SCIENCE
IN
CIVIL ENGINEERING

JANUARY 2010

Approval of the thesis:

CAPACITY RELATED PROPERTIES AND ASSESSMENT OF SCHOOL BUILDINGS IN TURKEY

submitted by **İLKER KALEM** in partial fulfillment of the requirements for the degree of **Master of Science in Civil Engineering Department, Middle East Technical University** by,

Prof. Dr. Canan Özgen
Dean, Graduate School of **Natural and Applied Sciences** _____

Prof. Dr. Güney Özcebe
Head of Department, **Civil Engineering** _____

Assoc. Prof. Dr. Ahmet Yakut
Supervisor, **Civil Engineering Dept., METU** _____

Examining Committee Members:

Assoc. Prof. Dr. Murat Altuğ Erberik
Civil Engineering Dept., METU _____

Assoc. Prof. Dr. Ahmet Yakut
Civil Engineering Dept., METU _____

Assoc. Prof. Dr. Cem Topkaya
Civil Engineering Dept., METU _____

Assist. Prof. Dr. Alp Caner
Civil Engineering Dept., METU _____

Yüksel İlkay Tonguç (M.S.)
PROMER Engineering _____

Date: _____

I hereby declare that all information in this document has been obtained and presented in accordance with academic rules and ethical conduct. I also declare that, as required by these rules and conduct, I have fully cited and referenced all material and results that are not original to this work.

Name, Last name: İlker Kalem

Signature :

ABSTRACT

CAPACITY RELATED PROPERTIES AND ASSESSMENT OF SCHOOL BUILDINGS IN TURKEY

Kalem, İlker

M.S., Department of Civil Engineering

Supervisor: Assoc. Prof. Dr. Ahmet Yakut

January 2010, 92 pages

Turkey is located on a seismically active region. Heavy damage observed in school buildings during recent earthquakes, revealed that seismic performance of school buildings is considerably poor. Therefore, determination of seismic vulnerability of these buildings has gained significant attention. Capacity curves that reflect properties of buildings are used to determine the seismic demand, thus, a decision can be made about the expected performance of the buildings. In addition, seismic vulnerability assessment procedures are also developed to assess the expected performance of buildings.

In this study, it was intended to determine capacity related properties of school buildings located in Turkey. Additionally, applicability of some existing seismic vulnerability assessment procedures for school buildings is investigated. The procedures developed by Yakut [3], Hassan & Sozen [8] and Ozcebe et al. [10] were employed. For this purpose, a set of school buildings that are believed to represent typical cases were employed. Nonlinear static analysis was carried out to determine the capacity related properties and approximate seismic demand. All buildings were assessed using the available

preliminary seismic assessment procedures and the results were compared with detailed assessment procedures.

Keywords: School buildings, capacity curve, capacity related properties and seismic vulnerability assessment procedures

ÖZ

TÜRKİYE'DEKİ OKUL BİNALARININ KAPASİTE İLİŞKİLİ ÖZELLİKLERİ VE DEĞERLENDİRİLMESİ

Kalem, İlker

Yüksek Lisans, İnşaat Mühendisliği Bölümü

Tez Yöneticisi : Doç. Dr. Ahmet Yakut

Ocak 2010, 92 sayfa

Türkiye sismik olarak aktif bir bölgede konumlanmıştır. Son depremlerde, okul binalarında ağır hasarların gözlenmiş olması, okul binalarının sismik performansının oldukça zayıf olduğunu göstermiştir. Bu nedenle, bu binaların sismik hasar görebilirliklerinin belirlenmesi önem kazanmıştır. Binaların özelliklerini yansıtan kapasite eğrisi, sismik talebi belirlemek için kullanılır; böylece, binaların beklenen performansı hakkında bir karar verilebilir. Ayrıca, binaların beklenen performansını değerlendirmek için sismik performans değerlendirme yöntemleri de geliştirilmiştir.

Bu çalışmada Türkiye'deki okul binalarının kapasite ilişkili özelliklerinin belirlenmesi amaçlanmıştır. Ayrıca, bazı sismik değerlendirme yöntemlerinin okul binaları için uygulanabilirliği araştırılmıştır. Yakut [3], Hassan & Sozen [8] ve Ozcebe vd. [10] tarafından geliştirilen yöntemler bu kapsamda kullanılmıştır. Bu amaçla, tipik özellikleri temsil ettiği kabul edilen bir grup okul binası incelenmiştir. Kapasite ilişkili özellikleri ve yaklaşık sismik talebi belirlemek için lineer olmayan statik analiz yöntemi kullanılmıştır. Tüm binalar mevcut sismik ön değerlendirme yöntemleri ile incelenmiş ve sonuçlar detaylı değerlendirme yöntemleriyle karşılaştırılmıştır.

Anahtar Sözcükler: Okul binaları, kapasite eğrisi, kapasite ilişkili özellikler ve sismik performans belirleme yöntemleri

To My Parents

ACKNOWLEDGMENTS

This study was conducted under the supervision of Assoc. Prof. Dr. Ahmet Yakut. I would like to express my sincere appreciation for his invaluable guidance, extensive support, advices, criticisms, and patience that he has provided me throughout the study. It was a great honor and pleasure for me to work with him.

I would like to express my sincere appreciation to structural mechanics division research assistant Abdullah Dilsiz for sharing his knowledge.

I would like to express my special thanks to Levent Mazılıgüney. He is always near me and his support helped me a lot during my master degree studies.

I also owe thanks to Emre Düzgün, Melisa Kızılkan, Özgür Yapar, Kerem Murat Özdemir and Başak Atak for their helps and support whenever I needed in this study.

I am grateful to my English teacher Hilal Dinçer for sharing her invaluable time, knowledge and support.

Last but not least, I would like to express my deepest appreciation to my parents -the most precious people in my life- for their confidence in me and for the support, love and understanding that they have provided me throughout my life.

TABLE OF CONTENTS

LIST OF TABLES

TABLES

LIST OF FIGURES

FIGURES

CHAPTER 1

INTRODUCTION

1.1 BACKGROUND

Turkey lies in one of the most seismically active regions in the world. In recent decades, earthquakes caused tens of thousands of deaths, huge amounts of economic losses and significant damage to buildings in Turkey. Recent observations after the Marmara (17 August 1999, M_w=7.4), Düzce (12 November 1999, M_w=7.2) and Bingöl (1 May 2003, M_w=6.4) earthquakes revealed that school buildings have been among the most severely damaged buildings. It has also been revealed that seismic performance of existing school buildings is inadequate, unfortunately, as evidenced by huge damage experienced by these buildings. Especially, the tragic collapse of the Çeltiksuyu Primary School Dormitory in Bingöl earthquake that killed 84 students and a teacher had striking evidence of how vulnerable these buildings were. Because of poor performance of school buildings in Turkey, researches focusing on determination of seismic vulnerability of these buildings have gained prominence. Capacity curves that reflect properties of buildings can be used to determine the seismic demand due to a given hazard represented by response spectrum. Based on this demand, a decision can be made about the expected performance of the building. In addition, seismic vulnerability assessment procedures that rely on capacity related properties of buildings can also be developed to assess the expected performance of such buildings.

Capacity curves are developed through parameters obtained with nonlinear analyses. Since they directly affect building vulnerability and

consequently the losses, the accuracy and reliability of these curves have a significant role on seismic loss estimation studies. They reflect features of the existing buildings. Capacity curves are recommended to be used in loss estimation, risk assessment and quick evaluation studies for reinforced concrete frame buildings. [1]

Researches become valuable as the prediction of the seismic vulnerability of existing buildings come into prominence. Seismic performance assessment procedures can be divided into three main categories in the literature. These are walk down (street survey), preliminary evaluation procedures and detailed assessment procedures.

Walk-down survey or street survey is the simplest and quickest way. Superficial data collected from a brief inspection of the building is sufficient. Typical parameters are the number of stories, vertical and plan irregularities, location of the building, age of the building, its structural system and apparent material and workmanship quality. Rapid evaluation techniques serve to identify or rank highly vulnerable buildings. These highly vulnerable buildings are investigated in detail. [3]

Preliminary assessment techniques are employed when a more detailed and reliable assessment than the walk-down survey is needed. In addition to the data collected for the walk-down survey procedures, the size and orientation of the structural components, material properties and layout are needed. [3, 5]

The detailed vulnerability assessment procedures, the third category among assessment procedures, involve the in-depth evaluation of the buildings. In addition to the available information, the geometrical properties of the components, mechanical properties of the materials, and detailing of the components are needed. Linear or non-linear analyses are also needed to determine the response quantities in these procedures. [3, 5].

Although comprehensive research devoted to reinforced concrete residential buildings yielded capacity curve parameters and seismic vulnerability assessment procedures for residential buildings in Turkey, similar endeavor has not been given to school buildings. Therefore, this study focuses

on determination of capacity curve parameters and validity of existing assessment procedures for school buildings in Turkey.

1.2 PREVIOUS WORK/LITERATURE SURVEY

In the sections that follow, previous studies on capacity related properties of reinforced concrete buildings will be summarized along with the preliminary seismic vulnerability assessment procedures developed for the buildings in Turkey.

1.2.1 Capacity Related Properties of RC Buildings

In the HAZUS (Hazard United States) [6] methodology, the capacity curves are used to determine seismic vulnerability. These capacity curves are composed according to the design codes and they are very idealistic. Moreover, these curves don't take into account the variations in the regional design practices. They are represented in the acceleration displacement response spectra (ADRS) format. The parameters such as fundamental period, yield over-strength ratio, post elastic stiffness, yield base shear coefficient, yield and ultimate drift ratios have been obtained from the idealized capacity curves. These parameters are used to determine seismic response of buildings under a given hazard level. [1]

A typical capacity curve recommended by HAZUS [6] representing building response by three segments is illustrated in Figure 1.1. In this curve, point A shows the code design point, point B represents actual elastic limit and point C shows the ultimate point beyond which the structure fails.

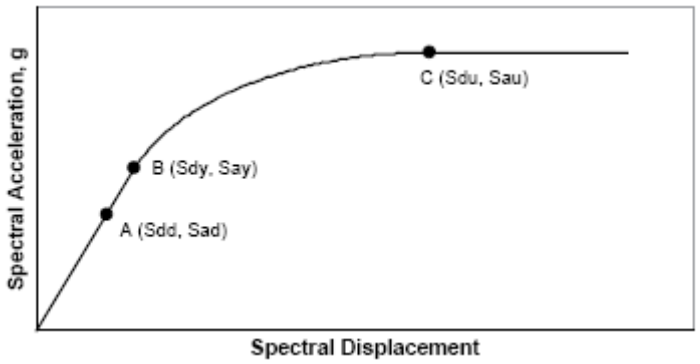

Figure 1.1 Capacity Curve as Described in HAZUS [6]

These points are obtained from Equations (1.1), (1.2), (1.3) and (1.4):

$$Sa_y = \frac{C_s \gamma}{\alpha_1} \tag{1.1}$$

$$Sd_y = \frac{Sa_y T_e^2 g}{4\pi^2} \tag{1.2}$$

$$Sa_u = \lambda Sa_y \tag{1.3}$$

$$Sd_u = \lambda \mu Sd_y \tag{1.4}$$

where

C_s : design strength coefficient (fraction of building weight)

γ : yield over-strength ratio

α : modal weight factor

T_e : effective building period

λ : ultimate over-strength ratio

μ : ductility ratio

Sa_y, Sa_u : Yield and ultimate spectral acceleration, respectively

Sd_y, Sd_u : Yield and ultimate spectral displacement, respectively

Up to yield (between Origin and Point B), the capacity curve is assumed to be linear. From yield to the ultimate point (between Point B and Point C), the capacity curve is assumed to be in the nonlinear range.

ATC-40 [30] and FEMA 356 [31] represent original capacity curve by an approximate bilinear curve as most of the approximate procedures do. Regional construction practice and design codes generally guide these capacity curves. HAZUS [6] uses capacity curves and fragilities that are derived from expert opinion based on the ideal building characteristics. These characteristics comply with the codes and also reflect properties of the existing buildings in the U.S. In addition, they are suitable for regions where the as-built and design properties of the existing buildings are similar. In case of poor code compliance, properties of existing buildings differ from the design values, which is generally the case for Turkish buildings as revealed by the major 1999 earthquakes. This calls for specific building properties to be used in their vulnerability analysis. Pushover analyses serve to obtain the capacity of a particular structure when structural information is available. Old existing buildings are usually deprived of this information. Regional vulnerability can be determined if similar buildings' capacity curves are obtained rather than a single buildings' capacity curve, just like loss estimation studies. [1]

A comprehensive study has been performed by Yakut [1] to obtain capacity related properties of reinforced concrete frame buildings in Turkey. In this study, thirty three sample buildings were selected to represent a typical subset of a comprehensive database consisting of nearly 500 buildings. All buildings were reinforced concrete frame structures with masonry infill walls and located in the highest seismic zone (Zone 1 and 2 according to TEC 1997) of Turkey. The number of stories of the buildings ranged from two to five. The statistical properties of all parameters needed to describe the capacity curve are given in Table 1-1 for each number of stories. [1]

Table 1-1 Statistics of Capacity Curve Parameters [1]

		Number of Stories			
Parameter		2	3	4	5
Sd_y (cm)	mean	0.75	1.06	1.67	1.52
	st. dev.	0.25	0.29	0.71	0.35
Sa_y (g)	mean	0.25	0.18	0.16	0.12
	st. dev.	0.09	0.07	0.04	0.04
Sd_u (cm)	mean	7.30	10.65	12.84	14.06
	st. dev.	1.50	2.65	3.61	5.40
Sa_u (g)	mean	0.28	0.21	0.18	0.14
	st. dev.	0.10	0.08	0.05	0.04
C_s	mean	0.10	0.10	0.10	0.10
	st. dev.	0.00	0.00	0.00	0.00
T_e	mean	0.27	0.34	0.47	0.55
	st. dev.	0.05	0.11	0.11	0.14
PF	mean	1.17	1.24	1.28	1.29
	st. dev.	0.02	0.04	0.02	0.01
α	mean	0.94	0.88	0.83	0.83
	st. dev.	0.02	0.06	0.05	0.03
γ	mean	2.31	1.58	1.30	1.02
	st. dev.	0.85	0.52	0.39	0.32
λ	mean	1.13	1.15	1.14	1.16
	st. dev.	0.04	0.12	0.03	0.06
μ	mean	9.23	9.26	7.67	7.86
	st. dev.	3.03	3.12	3.01	2.22

A number of attempts have also been made recently to recommend idealized capacity curves for the common building types in Turkey. A study conducted by Japan International Cooperation Agency (JICA) [22] and

Istanbul Metropolitan Municipality [22] focused on estimating losses from future earthquakes that are likely to impact Istanbul. The study idealized the capacity curves using the elasto-plastic approximation. These curves were obtained from the simplified analyses. A further study by Bogazici University [23] dealt with the earthquake risk assessment for the Istanbul region. The capacity curves were represented by elasto-plastic behavior similar to JICA study. The analyses performed by Yakut [1] were based on 3D modeling. However, both JICA and Bogazici University studies are the results of simpler analyses using certain approximations and assumptions.

1.2.2 Preliminary Seismic Assessment Procedures

The procedures developed by Yakut [3], Hassan & Sozen [8] and Ozcebe et al. [10] are some examples of the preliminary assessment procedures developed mainly for the reinforced concrete structures in Turkey.

1.2.2.1 *Yakut's Procedure* [3]

Yakut [3] developed a preliminary procedure to evaluate seismic performance of low- to mid-rise reinforced concrete buildings in Turkey. This procedure incorporates the following factors that are observed to be the main cause of damage in Turkey;

- Improper configuration of architectural and structural system
- Poor and inadequate detailing and proportioning
- Substandard construction quality due to lack of technical control and supervision

The shear capacity of each structural component is computed considering only the concrete contribution using Equation (1.5);

$$V_{c_i} = c\alpha f_{ctk} b_w h \tag{1.5}$$

where

V_{c_i} : shear capacity of a rectangular concrete member without web reinforcement

b_w, h : dimensions of the member considered

f_{ctk} : direct concrete tensile strength

α : combined effect of strength reduction factor and the shear-tensile strength relation (0.65 for Turkish Design Code for RC buildings)

c : member orientation factor

c is taken as 2/3 when the capacity in the longitudinal direction of the member is calculated, 1/3 in transverse direction and 1 for shear walls in their own plane.

The total shear capacity is found by adding the member capacities in the direction of each principal axis. Afterwards, the yield base shear capacity, V_y, can be obtained in Equation (1.6) for the buildings that have no infill walls;

$$V_y = \frac{\Sigma V_c}{0.95e^{0.125n}} \tag{1.6}$$

where

V_y : yield base shear capacity

n : number of stories

Considering the influence of infill walls, the yield base shear capacity is computed in Equation (1.7) for the buildings that have infill walls;

$$V_{yw} = V_y\left(46\frac{A_w}{A_{tf}} + 1\right) \tag{1.7}$$

where

A_w : total area of the filler walls

A_{tf} : total floor area of the building

From these values, the Basic Capacity Index (BCPI) called as yield over-strength ratio in the literature is calculated.

$$BCPI = \frac{V_y}{V_{code}} \tag{1.8}$$

where

V_{code} : the code base shear

The code base shear computed according to the design criteria in the code.

The BCPI is then modified with some factors that account for negative architectural features and the resulting value is called Capacity Index (CPI).

$$CPI = C_A C_M BCPI \tag{1.9}$$

$$C_A = 1 - (C_{AS} + C_{ASC} + C_{AP} + C_{AF}) \tag{1.10}$$

where

C_A : coefficient reflecting the architectural features

C_M : coefficient reflecting the construction quality

C_{AS} : coefficient reflecting the soft story features

C_{ASC} : coefficient reflecting the short column

C_{AP} : coefficient reflecting the effect of plan irregularity that results in horizontal torsion and significant amount of overhangs

C_{AF} : coefficient reflecting the vertical and in-plan discontinuity of frames

The penalty scores for this procedure are presented in Table 1-2 and recommended values of C_M are given in Table 1-3.

Table 1-2 Coefficients for Architectural Factors

Feature	Coefficients
Soft Story (C_{AS})	0.135
Short Column (C_{ASC})	0.052
Plan Irregularity (C_{AP})	0.055
Frame Irregularity (C_{AF})	0.035

Table 1-3 Recommended Values of C_M

Quality of construction and workmanship	C_M
Poor	$1-Q_r(1-C_A)$
Average	$1-Q_r(1-C_A)/3$
Good	1

Q_r ratios of either 0.44 or 0.55 are recommended for Turkey based on the field data and the extensive experience of bad construction. [3] In this thesis, the value of 0.44 was used. The capacity index values are, then, compared with some cut-off values to arrive at a final decision on the building safety. As reasonable limit value 1.2 is recommended.

1.2.2.2 Hassan and Sozen's Procedure **[8]**

This procedure aims to classify low-rise monolithic reinforced concrete structures in a given region according to their seismic vulnerability. This procedure requires the dimensions and locations of the structural elements and the floor area. It is based on two indices. One of these is the wall index (WI) obtained from Equation (1.11);

$$WI = \frac{A_{cw} + \left(\frac{A_{mw}}{10}\right)}{A_{ft}} \times 100 \qquad (1.11)$$

where

A_{cw} : total cross-section area of reinforced concrete walls in one horizontal direction at base

A_{mw} : total cross-section area of nonreinforced masonry filler walls in one horizontal direction at base

A_{ft} : total floor area above base in a building

The second index is the column index (CI) obtained using Equation (1.12);

$$CI = \frac{(A_{ce})}{A_{ft}} \times 100 \tag{1.12}$$

$$A_{ce} = \frac{A_{col}}{2} \tag{1.13}$$

A_{ce} : effective cross-sectional area of columns at base

A_{col} : total cross-sectional area of columns above base

A plot of these indexes is prepared such that the y-axis represents the wall index (WI) and the x-axis represents the column index (CI) as shown in Figure 1-2. The closer is the point located by the two indices to the origin, the more vulnerable is the building. Figure 1.3 shows the assessment carried out for the data obtained from 1992 Erzincan earthquake. The March 13, 1992 Erzincan earthquake event was rated to have a Richter surface magnitude of 6.8. Its epicenter was located at 39.7º latitude and 39.6º longitude. The estimated focal depth was 28 km. Maximum ground acceleration, recorded on alluvium with a depth of approximately 200 m, were 0.5G (E-W) and 0.4G (N-S). Maximum ground displacement, calculated in a direction parallel to the North Anatolia Fault (N 34 E), was 0.25 m. [34]

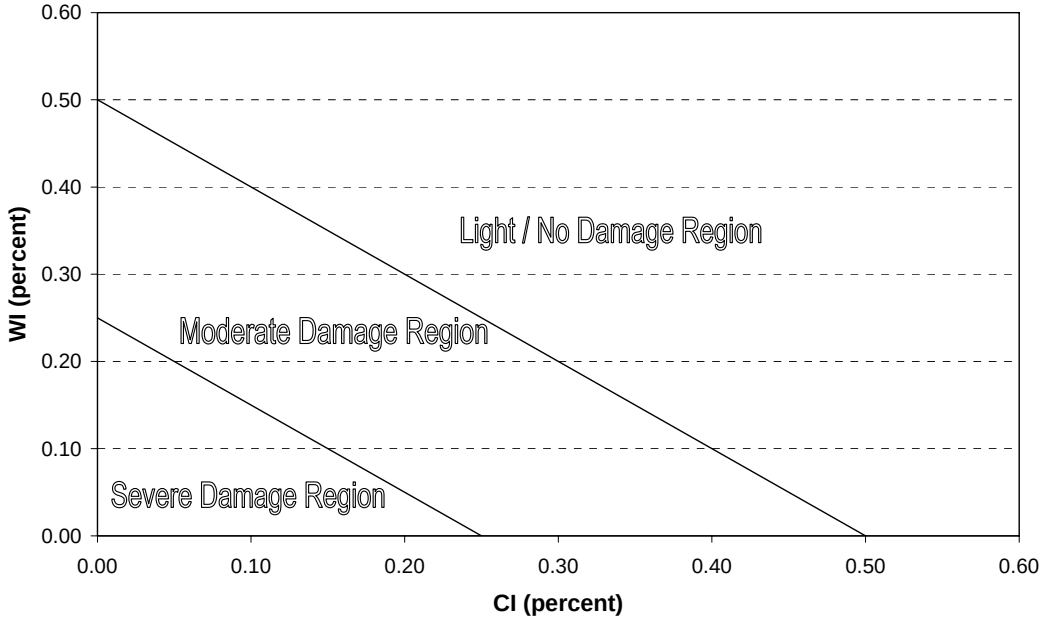

Figure 1.2 Proposed Evaluation Method

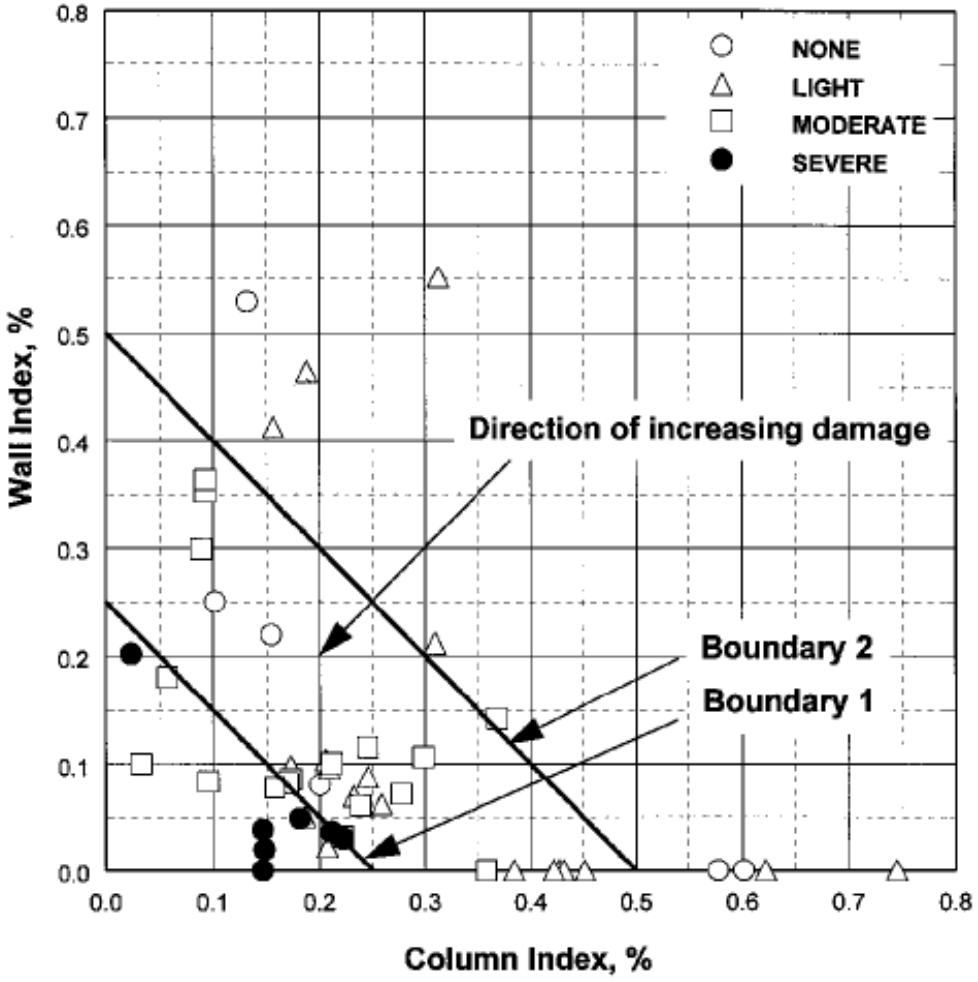

Figure 1.3 Assessment for Erzincan Database [8]

1.2.2.3 Ozcebe et al.'s Procedure [10]

This procedure that is based on a statistical model aims to identify the buildings that are highly vulnerable to earthquakes. The procedure is applicable to one- to seven-story reinforced concrete buildings. There are six parameters described below that are used in this methodology;

- Number of stories (n)
- Minimum normalized lateral stiffness index (mnlstfi)
- Minimum normalized lateral strength index (mnlsi)

- Normalized redundancy score (nrs)
- Soft story index (ssi)
- Overhang ratio (or)

1. Number of Stories (n): This is the total number of individual floor systems above the ground level.

2. Minimum Normalized Lateral Stiffness Index (mnlstfi): This index represents the lateral rigidity of the ground story, which is usually the most critical story. It is calculated by considering the columns and the structural walls at the ground story. The mnlstfi parameter shall be computed based on the following relationship;

$$mnlstfi = \min(I_{nx}, I_{ny}) \tag{1.14}$$

$$I_{nx} = \frac{\sum (I_{col})_x + \sum (I_{sw})_x}{\sum A_f} \times 1000 \tag{1.15}$$

$$I_{ny} = \frac{\sum (I_{col})_y + \sum (I_{sw})_y}{\sum A_f} \times 1000 \tag{1.16}$$

where, $\Sigma(I_{col})_x$ and $\Sigma(I_{col})_y$ are the summation of the moment of inertias of all columns about their centroidal x and y axes, respectively. $\Sigma(I_{sw})_x$ and $\Sigma(I_{sw})_y$ are the summation of the moment of inertias of all structural walls about their centroidal x and y axes, respectively. I_{nx} and I_{ny} are the total normalized moment of inertia of all members about x and y axes, respectively. ΣA_f is the total floor area above ground level.

3. Minimum Normalized Lateral Strength Index (mnlsi): It indicates the base shear capacity of the critical story. In the calculation of this index, unreinforced masonry filler walls are assumed to carry 10 percent of the shear force that can be carried by a structural wall having the same cross-sectional area. As in mnlstfi calculation, the vertical reinforced members with a cross-sectional aspect ratio of 7 or more are classified as structural walls. The mnlsi parameter shall be calculated by using the following Equation;

$$mnlsi = \min(A_{nx}, A_{ny}) \tag{1.17}$$

$$A_{nx} = \frac{\sum (A_{col})_x + \sum (A_{sw})_x + 0.1\sum (A_{mw})_x}{\sum A_f} \times 1000 \tag{1.18}$$

$$A_{ny} = \frac{\sum (A_{col})_y + \sum (A_{sw})_y + 0.1\sum (A_{mw})_y}{\sum A_f} \times 1000 \tag{1.19}$$

For each column with a cross-sectional area denoted by A_{col};

$$(A_{col})_x = k_x \times A_{col}\,,\ (A_{col})_y = k_y \times A_{col} \tag{1.20}$$

where; k_x=1/2 for square and circular columns; k_x=2/3 for rectangular columns with $b_x > b_y$; k_x=1/3 for rectangular columns with $b_x < b_y$; and k_y=1-k_x

For each shear wall with cross-sectional area denoted by A_{sw};

$$(A_{sw})_x = k_x \times A_{sw}\,,\ (A_{sw})_y = k_y \times A_{sw} \tag{1.21}$$

where; k_x=1 for structural walls in the directional of x-axis; k_x=0 for structural walls in the direction of y-axis; and k_y=1-k_x

For each unreinforced masonry filler wall with no window or door opening and having a cross-sectional area denoted by A_{mw};

$$(A_{mw})_x = k_x \times A_{mw}\,,\ (A_{mw})_y = k_y \times A_{mw} \tag{1.22}$$

where; k_x=1 for masonry walls in the direction of x-axis; k_x=0 for masonry walls in the direction of y-axis; and k_y=1-k_x

4. Normalized Redundancy Score (nrs): Redundancy is the indication of the degree of the continuity of multiple frame lines which distribute lateral forces throughout the structural system. The normalized redundancy ratio (nrr) of a frame structure is calculated by using the following expression;

$$nrr = \frac{A_{tr}(nf_x - 1)(nf_y - 1)}{A_{gf}} \tag{1.23}$$

where; A_{tr} is the tributary area for a typical column. A_{tr} shall be taken as 25 m^2 if nf_x and nf_y are both greater than and equal to 3. In all other cases, A_{tr} shall be taken as 12.5 m^2. nf_x, nf_y are the number of continuous frame lines in the critical story (usually the ground story) in x and y directions, respectively. A_{gf} is the area of the ground story, i.e. the footprint area of the building.

Depending on the value of nrr computed from Equation (1.23), the following discrete values are assigned to the normalized redundancy score (nrs):

nrs = 1 for $0 < nrr \leq 0.5$

nrs = 2 for $0.5 < nrr \leq 1.0$

nrs = 3 for $1.0 < nrr$

5. Soft Story Index (ssi): On the ground story, there are usually fewer partition walls than in the upper stories. This situation is one of the main reasons for the soft story formations. Since the effects of masonry walls are included in the calculation of mnlsi, soft story index is defined as the ratio of the height of first story (i.e. the ground story), H_1, to the height of the second story, H_2.

$$ssi = \frac{H_1}{H_2} \tag{1.24}$$

6. Overhang Ratio (or): In a typical floor plan, the area beyond the outermost frame lines on all sides is defined as the overhang area. The summation of the overhang area of each story, $A_{overhang}$, divided by the area of the ground story, A_{gf}, is defined as the overhang ratio.

$$or = \frac{A_{overhang}}{A_{gf}} \tag{1.25}$$

Performance Classification: The damage index or the damage score corresponding to the life safety performance classification (DI_{LS}) shall be computed from the discriminant function described below;

$$DI_{LS} = 0.620n - 0.246mnlstfi - 0.182mnlsi - 0.699nrs + 3.269ssi + 2.728or - 4.905 \tag{1.26}$$

In the case of immediate occupancy performance classification (IOPC), the discriminant function, where DI_{IO} is the damage score corresponding to IOPC, based on these variables is;

$$DI_{IO} = 0.808n - 0.334mnlstfi - 0.107mnlsi - 0.687nrs + 0.508ssi + 3.884or - 2.868 \tag{1.27}$$

After determination of the DI_{LS} and DI_{IO} values, cutoff values based on number of stories for each performance classification is obtained;

$$CV_{LS} = CMC \times (-0.090n^3 + 1.498n^2 - 7.518n + 11.885) \quad (1.28)$$

$$CV_{IO} = CMC \times (-0.085n^3 + 1.416n^2 - 6.951n + 9.979) \quad (1.29)$$

The CMC values that are based on soil classification and distance are given in Table 1.4.

Table 1-4 Variation of CMC Values with Soil Type and Distance to Fault

Soil Classification (JICA)	Shear Wave Velocity (m/s)	Distance to Fault (km)				
		0-4	5-8	9-15	16-25	>26
B	>760	0.778	0.824	0.928	1.128	1.538
C	360-760	0.864	1.000	1.240	1.642	2.414
D	180-360	0.970	1.180	1.530	2.099	3.177
E	<180	1.082	1.360	1.810	2.534	1.900

By comparing the CV values with associated DI values, the performance grouping of the building for life safety performance classification and immediate occupancy performance classification are calculated as follows:

If $DI_{LS} > CV_{LS}$ take $PG_{LS} = 1$

If $DI_{LS} < CV_{LS}$ take $PG_{LS} = 0$

If $DI_{IO} > CV_{IO}$ take $PG_{IO} = 1$

If $DI_{IO} < CV_{IO}$ take $PG_{IO} = 0$

To decide the probable expected performance level of the building, the damage scores should be compared with the story dependent cutoff values. In each case, the building under evaluation is assigned an indicator variable of “0” or “1”. The indicator variable “0” corresponds to “none, light or moderate damage” in the case of LSPC and “none or light damage” in the case of IOPC. Similarly, the indicator variable “1” corresponds to “severe damage or collapse” in the case of LSPC and “moderate or severe damage or collapse” in

the case of IOPC. In the final stage, the building is rated in the "low risk group" if both indicator values are zero or in the "high risk group" when both indicator values are equal to unity. In all other cases buildings are classified as the cases "requiring further investigation" that indicates that these buildings generally lie in the "moderate risk group." [10]

1.2.3 Displacement Coefficient Method

An advanced approach for determining seismic vulnerability is based on approximate determination of the displacement demand, generally called as target displacement. This displacement can then be compared with the capacity curve to determine the expected seismic performance. The target displacement can be computed using a widely employed method that is displacement coefficient method. Displacement coefficient method aims to determine a target displacement from the elastic displacement through modification factors. The effective fundamental period, T_e, and target displacement, δ_t, are calculated as;

$$T_e = \sqrt{\frac{K_i}{K_e}} T_i \tag{1.30}$$

$$\delta_t = C_0 C_1 C_2 C_3 S_a \frac{T_e^2}{4\pi^2} g \tag{1.31}$$

where

C_0 : coefficient that converts SDOF spectral displacement to MDOF roof displacement (elastic)

The values for modification factor C_0 are presented in Table 1-5. [13]

Table 1-5 Values for Modification Factor C_0

Number of Stories	C_0
1	1.0
2	1.2
3	1.3
5	1.4
10+	1.5

C_1 : expected maximum inelastic displacement divided by elastic displacement

$$C_1 = 1 + \frac{R-1}{aT_e^2} \tag{1.32}$$

$$C_1 = \begin{cases} C_1(T = 0.2s), T < 0.2s \\ 1.0, T > 1.0s \end{cases}$$

In this equation, a is 130, 90 and 60 for soil site B, C and D, respectively.

$$R = \frac{S_a}{V_y / W} C_m \tag{1.33}$$

The values for effective mass factor (C_m) are presented in Table 1-6. [13]

Table 1-6 Values for Effective Mass Factor (C_m)

Number of Stories	Concrete Frame	Concrete Shear Wall
1-2	1.0	1.0
≥3	0.9	0.8

C_2 : coefficient that incorporates the effects of pinched hysteretic shape, stiffness degradation and strength deterioration

$$C_2 = 1 + \frac{1}{800}\left(\frac{R-1}{T}\right)^2 \tag{1.34}$$

$$C_2 = \begin{cases} C_2(T = 0.2s), T < 0.2s \\ 1.0, T > 0.7s \end{cases}$$

C_3 : factor that reflects the increased displacements due to dynamic P-Δ effects

$$C_3 = \begin{cases} 1.0, \alpha \geq 0 \\ 1 + \dfrac{\alpha(R-1)^{3/2}}{T_e}, \alpha < 0 \end{cases}$$

The target displacement computed from Equation (1.31) can be used along with the capacity curve to approximately determine the expected seismic performance of the building. For this, the capacity curve of the building is represented by an idealized bilinear curve as shown in Figure 1.4. The idealization can be done using the approach proposed in FEMA 356 [31] as depicted in Figure 1.4 where the intersection of the idealized curve and the actual curve occurs at base shear value that is equal to $0.6V_y$, V_y being the yield base shear of the idealized curve. The area under both curves must approximately be the same. After the idealization of the curve, performance limits are computed by considering yield displacement and ultimate displacement to determine the seismic performance of the building. The ultimate displacement is accepted to be the limiting value for the collapse prevention performance level. The displacement limit for life safety performance is assigned the third quartile of the ultimate displacement. The yield displacement is accepted to be the limiting value for the immediate occupancy performance level. Then, the target displacement is compared with the calculated performance limits and the expected seismic performance of the building is determined.

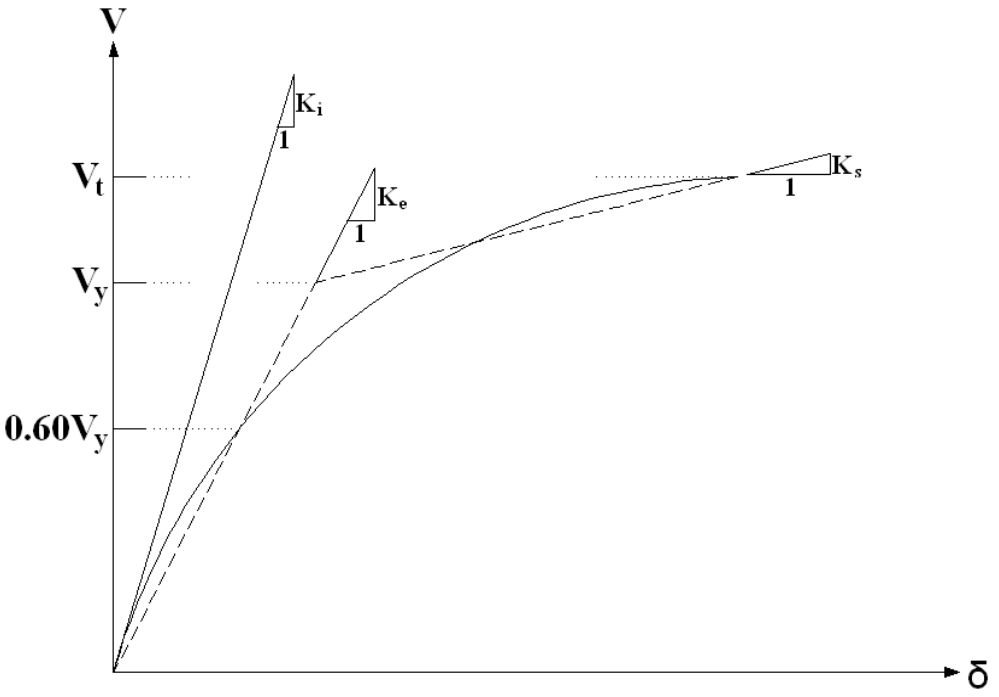

Figure 1.4 Idealized Force-Displacement Curve

1.3 OBJECT AND SCOPE

There are two primary aims of this study: 1) to determine capacity related properties of school buildings located in Turkey, 2) to investigate the applicability, on school buildings, of existing seismic vulnerability assessment procedures developed for residential buildings in Turkey.

The thesis is composed of four main chapters. First chapter gives a general overview of the study and brief information about capacity curves, preliminary seismic assessment procedures and displacement coefficient method.

Chapter 2 includes the description and analysis of buildings. In this chapter, properties of building inventory such as description of the database, general properties about selected buildings are given. Nonlinear static analysis results and dynamic properties of the buildings are also presented.

Chapter 3 includes results of existing assessment procedures, displacement coefficient method and their comparisons.

Finally, Chapter 4 is devoted to summary and conclusions. Recommendations are also given for future studies.

CHAPTER 2

DESCRIPTION AND ANALYSIS OF BUILDINGS

2.1 PROPERTIES OF BUILDING INVENTORY

2.1.1 Description of Building Database

Turkey is an earthquake-prone country. Strong earthquakes have led to significant damage of many school buildings in the past. Because of unexpected consequences, the government officials have initiated some projects to reduce seismic vulnerability of existing school buildings. Within this endeavor, Istanbul is given a special emphasis because of probability of a major potential earthquake in coming years. The Governorship of Istanbul has established an administrative unit to manage Istanbul Seismic Risk Mitigation and Emergency Preparedness Projects (ISMEP). This project is a significant attempt to implement essential principals of comprehensive disaster management financed by the World Bank. The main goals are to improve preparedness for a potential earthquake and retrofit or reconstruct of priority public buildings in Istanbul. ISMEP project consists of three components:

- Component A: Enhancing Emergency Preparedness
- Component B: Seismic Risk Mitigation for Priority Public Buildings
- Component C: Enforcement of Building Codes [20]

In this thesis, thirty three representative reinforced concrete school buildings that were selected from the inventory of school buildings contained in the ISMEP project were investigated. Of these, twenty eight buildings

(BLD1 - BLD28) were used to determine capacity related properties of school buildings and five buildings (BLD29 - BLD33) were employed to determine applicability of preliminary seismic assessment procedures for school buildings. These buildings were selected according to the number of stories, plan area, compressive concrete strength, shear wall density (percent) and basic capacity index (BCPI) proposed by Yakut [3]. The number of stories of the buildings ranged from three to five. Four-story buildings dominated the set. Figure 2-1 presents building statistics related to the number of stories. The plan area of the buildings displayed in Figure 2-2 was between 300-800 m^2. Distribution of compressive concrete strength shown in Figure 2-3 reveals that the compressive concrete strength was generally between 7-18 MPa with an average value of approximately 12 MPa. The structural system of the buildings was made of reinforced concrete with varying percentage of the column and shear wall area. The shear wall densities presented in Figure 2-4 is the minimum value of the shear wall area divided by the total floor area above the ground floor level corresponding to the two directions of the building. Most of the buildings had no shear walls. The percent of shear wall density was generally 0.25 in the shear wall structural system. Lastly, basic capacity index (BCPI) calculated in the more vulnerable direction for these buildings was between 0.25-2.00 (Figure 2-5).

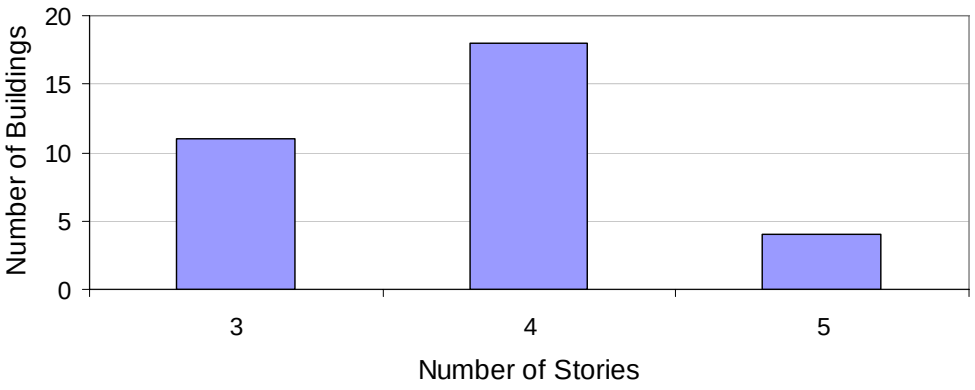

Figure 2.1 Distribution of Number of Stories

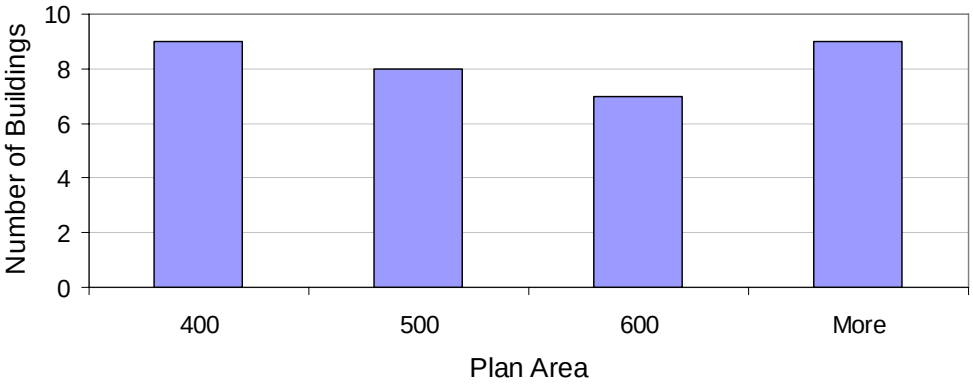

Figure 2.2 Distribution of Plan Area

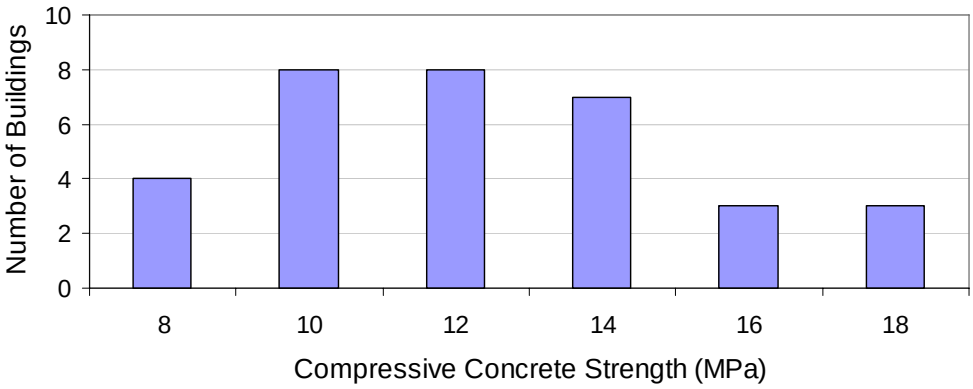

Figure 2.3 Distribution of Compressive Concrete Strength

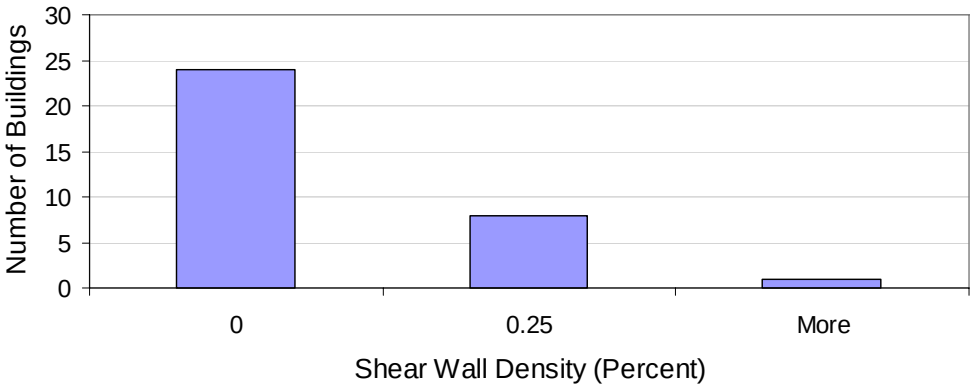

Figure 2.4 Distribution of Shear Wall Density (Percent)

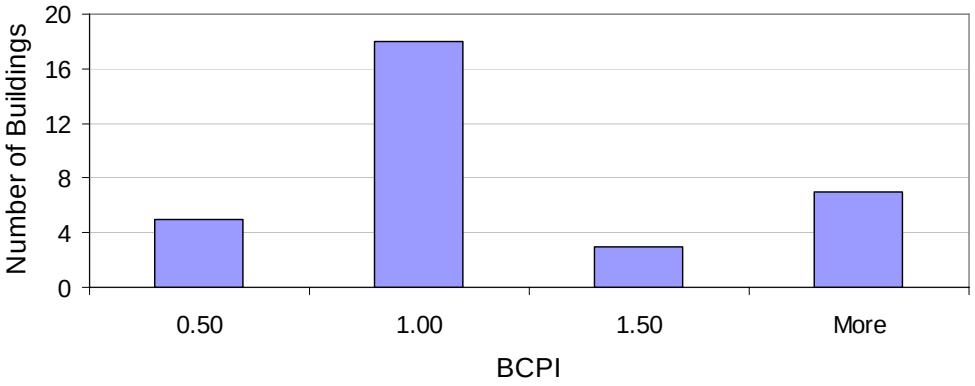

Figure 2.5 Distribution of Basic Capacity Index

2.1.2 General Properties of Selected Buildings

Twenty eight buildings that were selected to determine capacity related properties were located in Istanbul, Turkey. The remaining five buildings were located in Afyon, Izmir and Kutahya, Turkey. Six buildings were located in the highest seismic zone of Turkey and the remaining twenty seven being in the second highest seismic zone according to the current seismic zone map. General properties of selected buildings are presented in Table 2-1. Detailed properties of these buildings are summarized in Table A.1-1 of Appendix A. Figures 2-6 and 2-7 show period versus story number relationship and period versus height relationship for the buildings, respectively. Despite a large scatter of the period with respect to the number of stories, a reasonable trend is observed with respect to the building height. The equation given in the Turkish earthquake code ($T=0.07H^{3/4}$) seems to not adequately represent the distribution for the selected buildings (Figure 2-7).

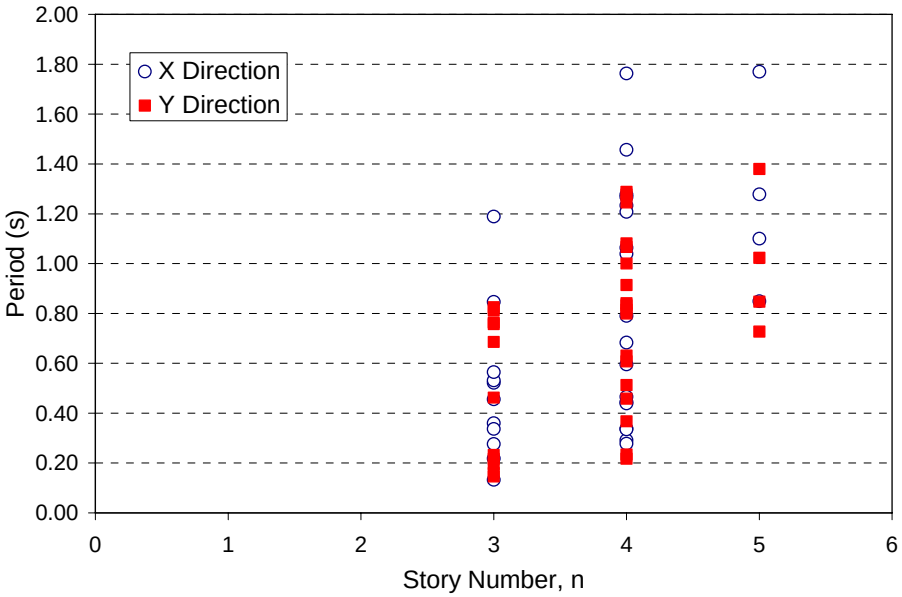

Figure 2.6 Period versus Story Number Relationship

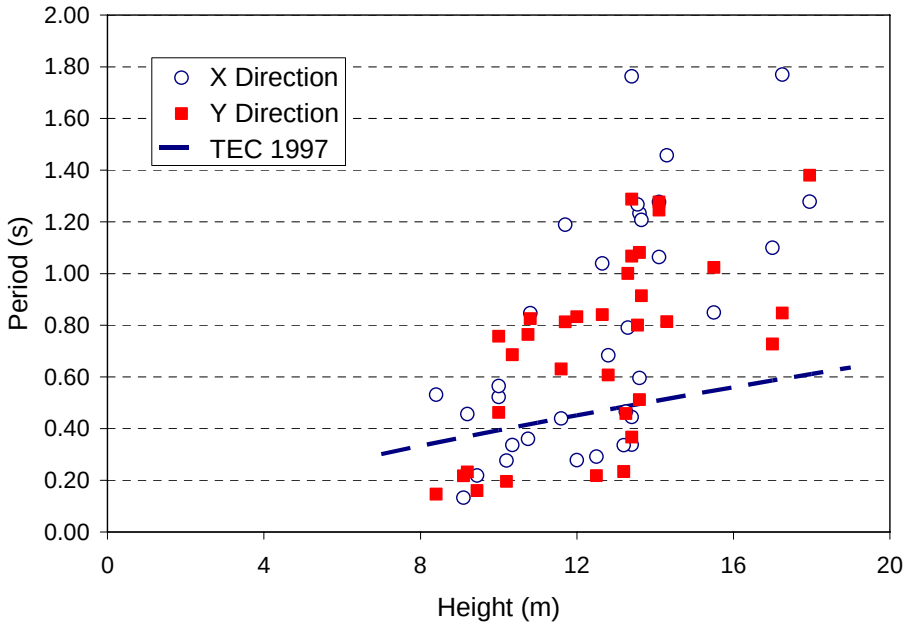

Figure 2.7 Period versus Height Relationship

Table 2-1 General Properties of Selected Buildings

Building ID	Location	No. of Stories	EQ Region	Plan Area (m^2)	Height (m)	Concrete Strength (Mpa)
BLD1	Istanbul/Bahcelievler	4	2	595	12.50	9.70
BLD2	Istanbul/Bayrampasa	3	2	435	11.70	16.00
BLD3	Istanbul/Bayrampasa	4	2	335	12.80	11.20
BLD4	Istanbul/Bayrampasa	4	2	655	13.60	10.80
BLD5	Istanbul/Eminonu	5	1	356	15.50	13.60
BLD6	Istanbul/Eminonu	5	2	653	17.95	12.00
BLD7	Istanbul/Eminonu	3	1	315	10.00	10.70
BLD8	Istanbul/Eminonu	4	1	475	13.65	13.20
BLD9	Istanbul/Eminonu	4	1	540	14.10	10.50
BLD10	Istanbul/Esenler	4	2	425	13.40	14.70
BLD11	Istanbul/Esenler	3	2	320	8.40	12.00
BLD12	Istanbul/Fatih	3	2	780	10.75	8.80
BLD13	Istanbul/Fatih	3	2	630	10.35	18.20
BLD14	Istanbul/Fatih	4	2	410	14.30	14.00
BLD15	Istanbul/Fatih	4	2	650	13.30	12.80
BLD16	Istanbul/Fatih	5	2	505	17.25	16.50
BLD17	Istanbul/Fatih	4	2	700	13.25	17.70
BLD18	Istanbul/Fatih	4	2	545	14.10	13.30
BLD19	Istanbul/Fatih	3	2	322	9.10	7.10
BLD20	Istanbul/Fatih	4	2	520	12.00	8.00
BLD21	Istanbul/Fatih	3	2	355	10.00	8.50
BLD22	Istanbul/Gaziosmanpasa	5	2	495	17.00	11.20
BLD23	Istanbul/Gaziosmanpasa	3	2	430	9.45	9.60
BLD24	Istanbul/Gaziosmanpasa	4	2	555	12.65	9.80
BLD25	Istanbul/Gaziosmanpasa	4	2	413	13.40	9.50
BLD26	Istanbul/Gaziosmanpasa	4	2	425	11.60	12.80
BLD27	Istanbul/Kagithane	4	2	625	13.55	14.20
BLD28	Istanbul/Kagithane	4	2	310	13.40	7.00
BLD29	Afyon/Merkez	3	2	260	10.20	10.40
BLD30	Izmir/Konak	3	1	355	9.20	9.30
BLD31	Afyon/Merkez	4	2	800	13.60	8.30
BLD32	Izmir/Torbalı	4	1	800	13.20	12.30
BLD33	Kutahya/Tavsanlı	3	2	560	10.81	7.00

2.2 MODELING AND ANALYSIS

2.2.1 Modeling Using SAP2000 Software and Assumptions

The structural analysis program SAP2000 is a software package developed by Computers and Structures Inc. [32]. It is based on the finite element method for modeling and analysis. In this program, a frame element is modeled as a line element that has linearly elastic properties. The nonlinear force-displacement characteristics of individual frame elements are modeled as hinges represented by a series of straight line segments. A generalized force-deformation relationship for hinges used in pushover analysis is shown in Figure 2-8.

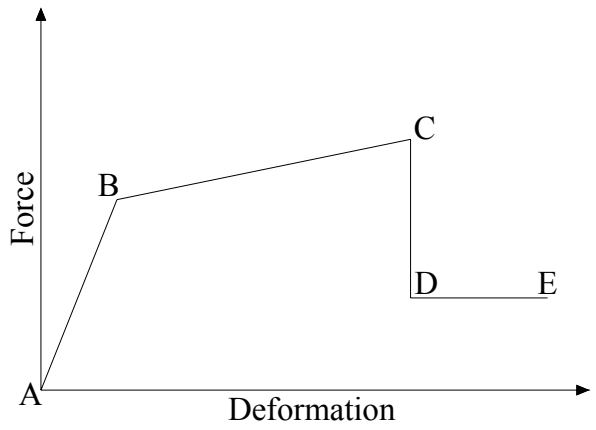

Figure 2.8 Generalized Force-Deformation or Moment-Rotation Relationship

Point A represents the origin (unloading condition) and point B represents the yielding state. Point C corresponds to the ultimate strength, where significant strength degradation begins. The drop from C to D represents the initial failure of the element. Point D corresponds to the residual strength and point E represents total failure.

There are three types of hinge properties in SAP2000 [32]. These are default hinge properties, user-defined hinge properties and generated hinge properties. Only default hinge properties and user-defined hinge properties can be assigned to frame elements.

Since the default properties are section dependent, default hinge properties can not be modified. When default hinge properties are used, the program combines its built-in default criteria with the defined section properties for each element. The built-in default hinge properties are typically based on ATC-40 [30] and FEMA-356 [31] criteria. User-defined hinge properties can either be based on default properties or be fully user-defined. When user-defined properties are not based on default properties, the hinge properties can be modified.

For user-defined hinge properties, the moment-curvature relations are converted into moment-rotation relations using the following Equations:

$$\theta_y = \frac{\phi_y . L}{6} \tag{2.1}$$

In this equation; L is member length, ϕ_y is curvature at yield and θ_y is rotation at yield.

Plastic hinge rotation capacity of members is estimated using the Equation (2.2) proposed by ATC-40 [30].

$$\theta_p = (\phi_{ult} - \phi_y) L_p \tag{2.2}$$

In this equation; L_p is plastic hinge length, ϕ_y is curvature at yield, ϕ_{ult} is ultimate curvature and θ_p is plastic rotation.

ATC-40 [30] suggests that plastic hinge length equals to half of the cross-section depth (L_p= h/2).

In this study, default-PMM hinges for columns and default-M3 hinges for beams were used.

Stiffness of concrete members is defined by considering cracked concrete sections. The cracked section stiffness of beams are taken as 40% of uncracked section stiffness and cracked section stiffness of columns and shear walls are calculated according to their axial load level:

Beams : $0.40\ (EI)_o$ (2.3)

Column and Shear Wall : $0.40\ (EI)_o$ if $N_D / (A_c f_{cm}) \leq 0.1$ (2.4a)

: $0.80\ (EI)_o$ if $N_D / (A_c f_{cm}) \geq 0.4$ (2.4b)

N_D is the axial load under gravity loading, A_c is the gross section area, f_{cm} is the existing concrete compressive strength, E is the modulus of elasticity and I is the uncracked moment of inertia. In this study, the cracked section stiffness of columns and shear walls are assumed to be 65% of uncracked section stiffness.

Rigid floor diaphragms were assigned at each story level and mass of the frames was lumped at the mass center of each story.

2.2.2 Linear Analysis

Total equivalent seismic load (base shear) acting on the entire building in the earthquake direction considered was determined according to Turkish earthquake code (TEC 2007) [33]. Then, the total equivalent seismic load was distributed to stories of the buildings as inverted triangular lateral load. The distributed loads were applied to the mass centers at each story of the building. The buildings were then analyzed to calculate elastic forces and displacements.

2.2.3 Nonlinear Static Analysis

Nonlinear static analysis, or pushover analysis, has been developed over the past twenty years. Since the procedure is relatively simple and considers post-elastic behavior, it has become the preferred analysis procedure for design and seismic performance evaluation. Pushover analysis is the process of pushing the structure laterally with a predefined lateral load pattern in increments until the structure reaches its ultimate deformation state.

The purpose of the pushover analysis is to evaluate the expected performance of a structural system by estimating its strength and deformation demands under design earthquakes by means of a static inelastic analysis and

comparing these demands to available capacities at the performance levels of interest. [24]

The general sequence of steps involved in performing pushover analysis can be summarized as follows:

1. The model of the structure is created.
2. Load-deformation diagrams of all important members that affect lateral response are defined.
3. Gravity loads composed of dead loads and a specified portion of live loads are applied to the structural model initially.
4. A predefined lateral load pattern which is distributed along the building height is applied.
5. Lateral loads are increased until member or some members yield under the combined effects of gravity and lateral loads.
6. Base shear and roof displacement are recorded at first yielding.
7. The structural model is modified to account for the reduced stiffness of yielded member or members.
8. A new lateral load increment (ΔF) is applied to the modified structural model such that additional member or members yield.
9. The lateral load increment (ΔF) and the roof displacement increment (ΔU) are added to the corresponding previous total values to obtain the accumulated values of the base shear and the roof displacement.
10. Steps 7, 8 and 9 are repeated until the roof displacement reaches a certain level of deformation or the structure becomes unstable.
11. The base shear is plotted versus the roof displacement to get pushover curve of the structure (Figure 2-9).

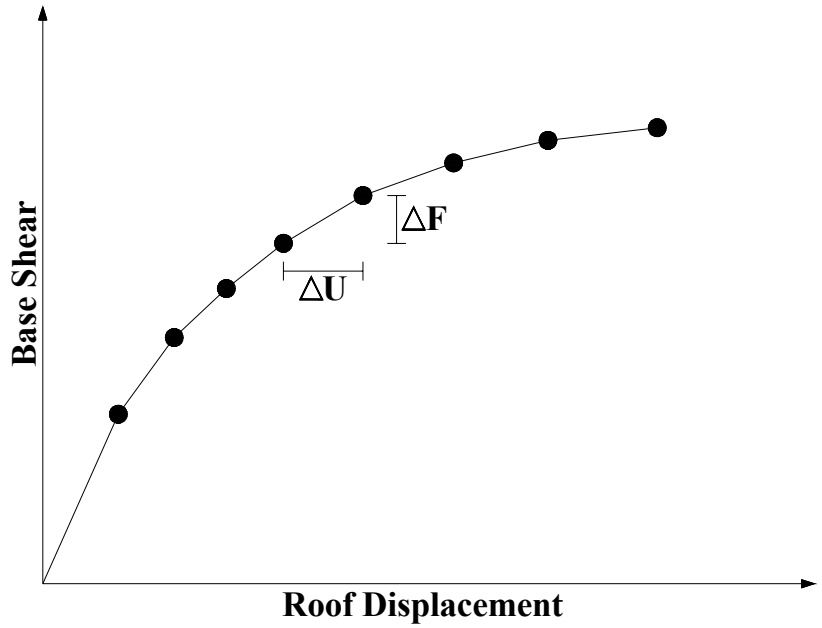

Figure 2.9 Pushover Curve of Structure

The procedure outlined above was used to carry out pushover analyses to obtain the capacity curve of the buildings.

2.3 RESPONSE OF BUILDINGS FROM PUSHOVER ANALYSIS

Three-dimensional models of all the selected buildings were prepared in the SAP2000 program. Nonlinear static analyses were conducted and pushover curves were determined for the buildings. Then, the buildings were grouped by considering the damage sequence. The corresponding plastic hinge patterns at significant yielding and ultimate capacity states are shown in the following figures. The symbols used for hinges indicate whether the yielding is at an initial level (in the vicinity of point B in Figure 2-8), major (on portion BC in Figure 2-8) or exceeds the failure initiation state (on portion DE in Figure 2-8). The buildings were pushed both in the longitudinal and transverse direction. However, the damage sequence was obtained only in longitudinal

direction (not necessarily the weak direction). There are three groups considering the damage sequence of the selected buildings. Figures 2-10, 2-14 and 2-19 present the plan layout of sample buildings in each group.

It can be observed from Figures 2-11, 2-12 and 2-13 that the damage sequence in Group-1 Buildings starts with the yielding of beam ends at the lower stories and upper stories and finally with the yielding of column bases. This is an expected sequence in achieving a ductile beam mechanism.

The damage sequence in Group-2 Buildings observed from Figures 2-15, 2-16, 2-17 and 2-18 starts with the yielding of column bases at the lower stories, then the yielding of column bases at the upper stories and finally with the yielding of beam ends at the lower stories. This is an undesirable sequence. It can be concluded that the beams are stronger than the columns.

Lastly, the damage sequence in Group-3 Buildings observed from Figure 2-20, 2-21, 2-22, 2-23 and 2-24 starts with the yielding of both column and beam ends at the lower stories simultaneously, then at the upper stories.

Sample pushover curves of the representative buildings in the longitudinal direction (x direction) for each group are displayed in Figures 2-25, 2-26 and 2-27.

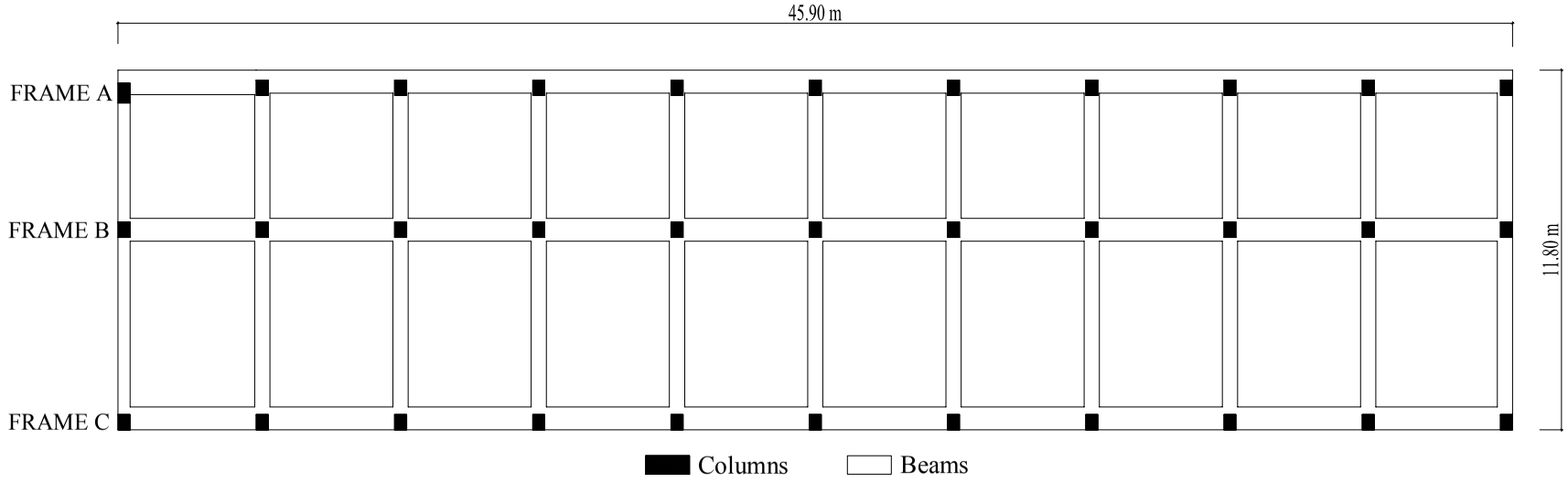

Figure 2.10 Plan Layout of the Selected Building for Group-1

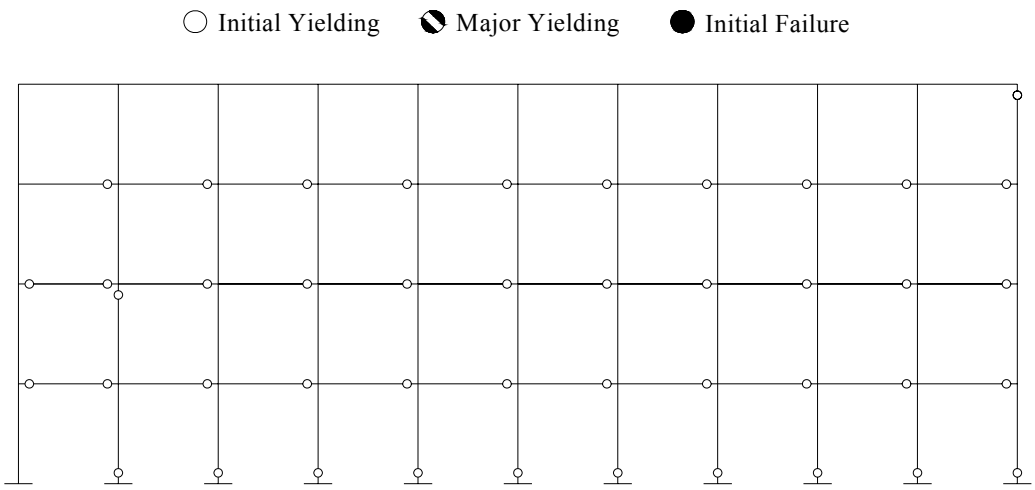

Figure 2.11a Hinge Patterns at Significant Yield for Group-1

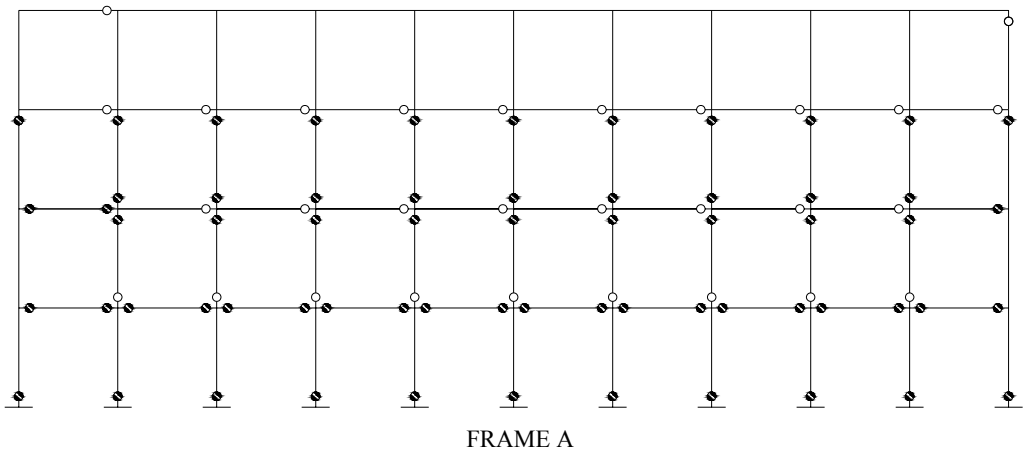

Figure 2.11b Hinge Patterns at the Ultimate Capacity for Group-1

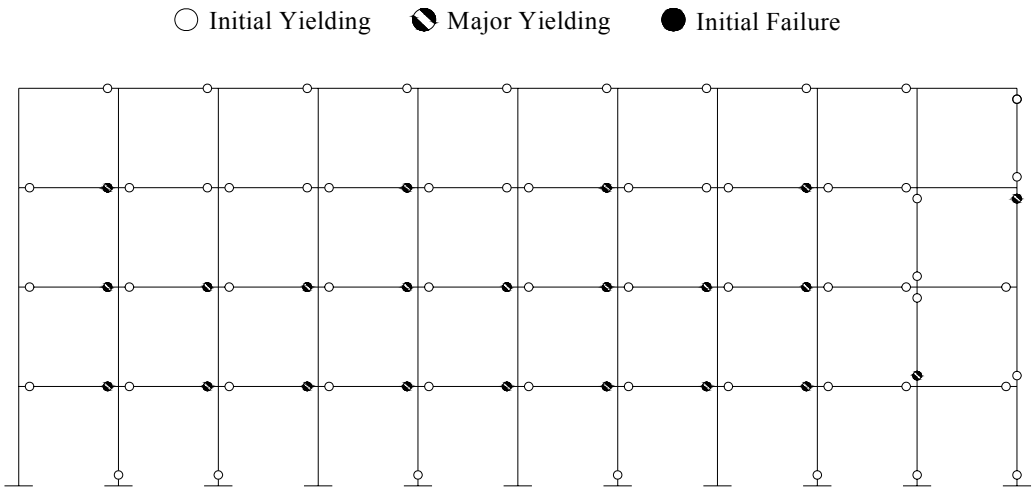

Figure 2.12a Hinge Patterns at Significant Yield for Group-1

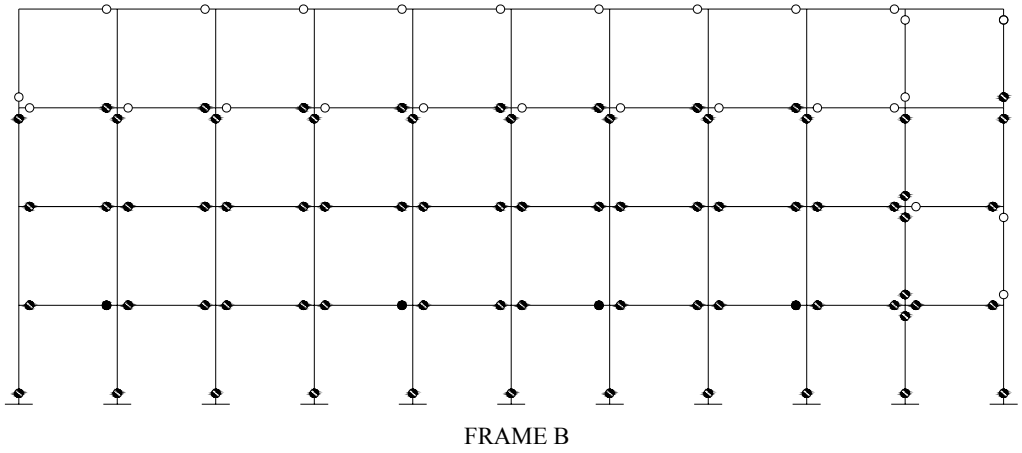

Figure 2.12b Hinge Patterns at the Ultimate Capacity for Group-1

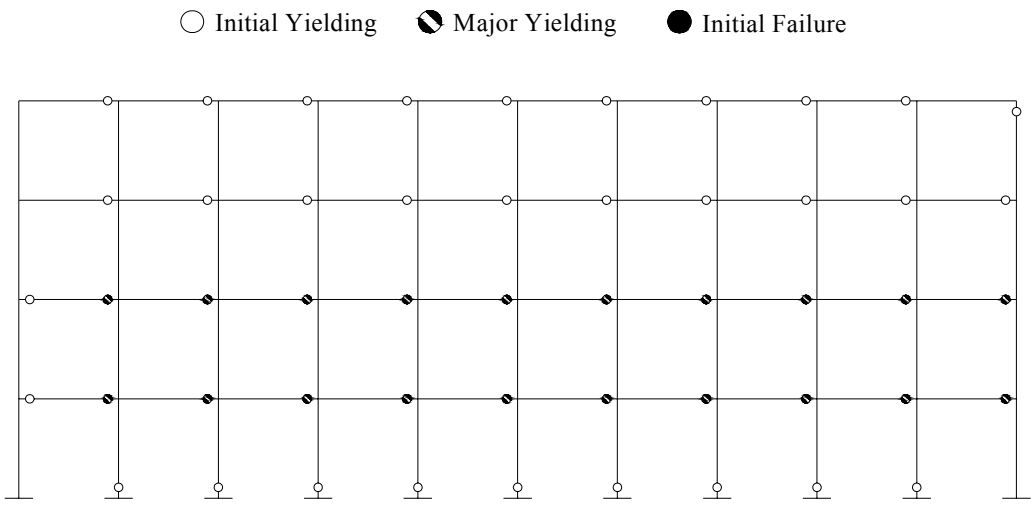

Figure 2.13a Hinge Patterns at Significant Yield for Group-1

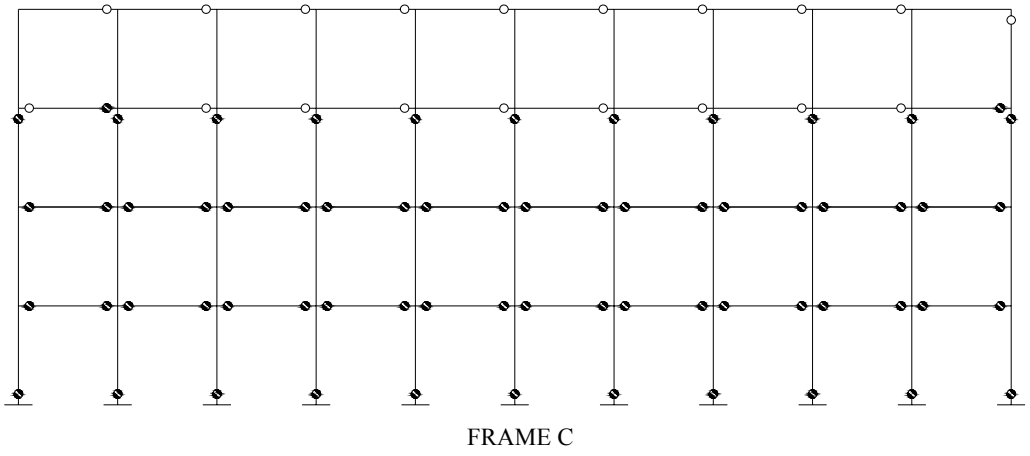

Figure 2.13b Hinge Patterns at the Ultimate Capacity for Group-1

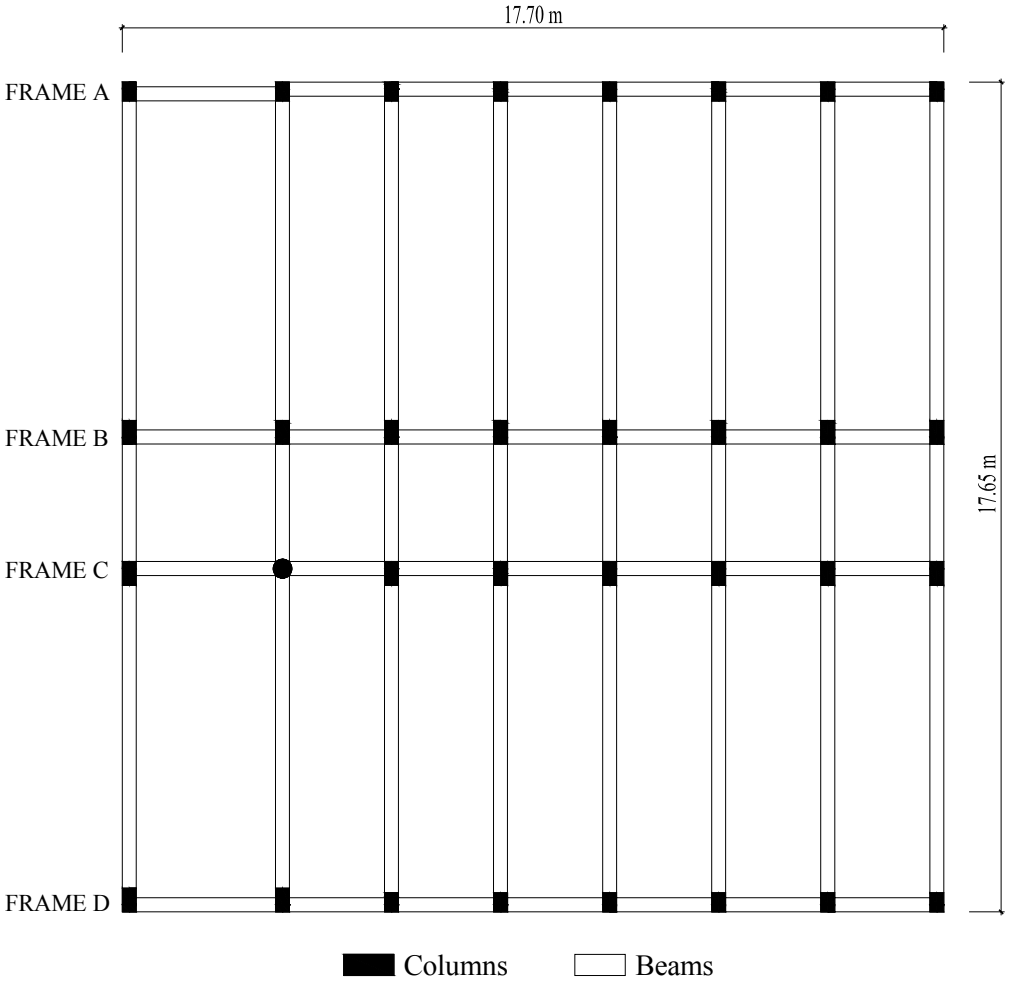

Figure 2.14 Plan Layout of the Selected Building for Group-2

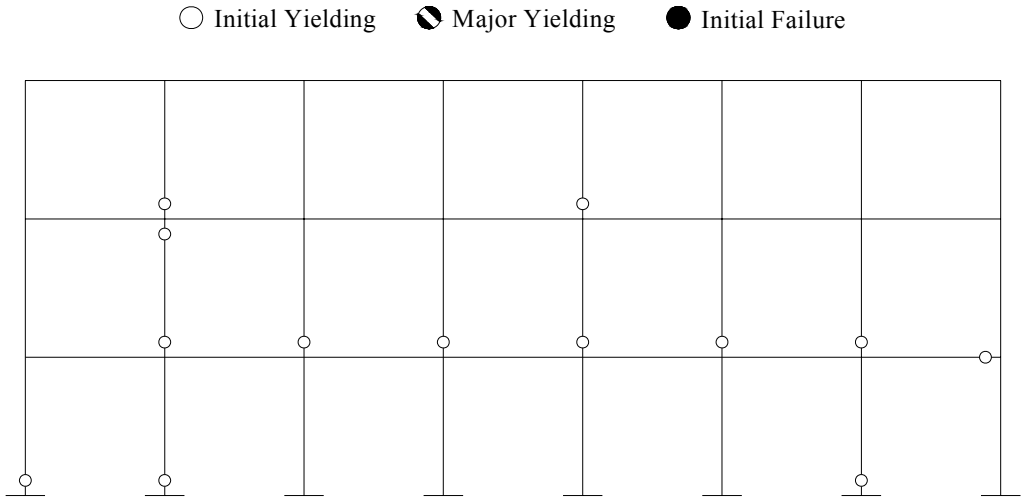

FRAME A

Figure 2.15a Hinge Patterns at Significant Yield for Group-2

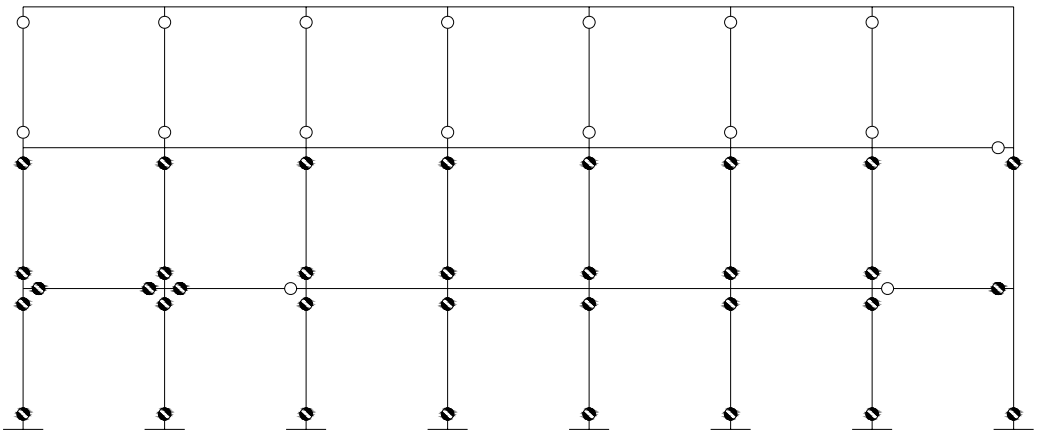

FRAME A

Figure 2.15b Hinge Patterns at the Ultimate Capacity for Group-2

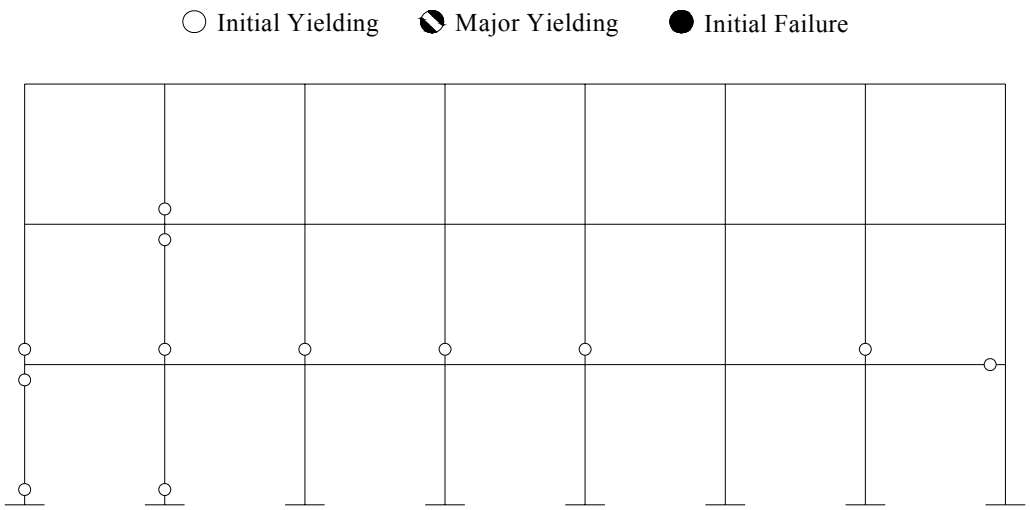

FRAME B

Figure 2.16a Hinge Patterns at Significant Yield for Group-2

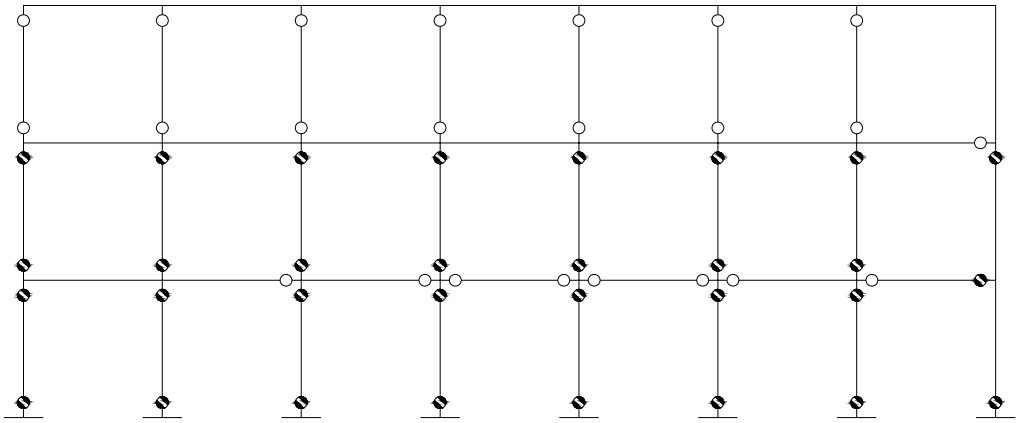

FRAME B

Figure 2.16b Hinge Patterns at the Ultimate Capacity for Group-2

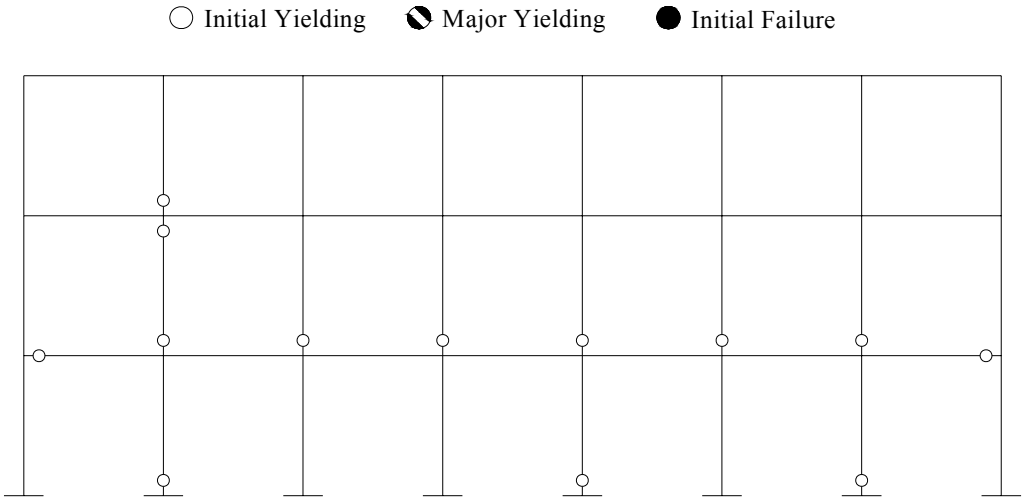

FRAME C

Figure 2.17a Hinge Patterns at Significant Yield for Group-2

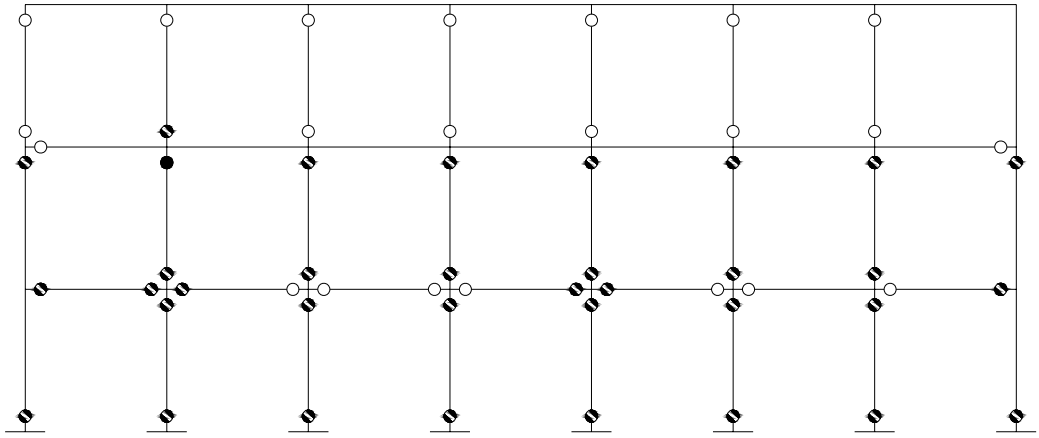

FRAME C

Figure 2.17b Hinge Patterns at the Ultimate Capacity for Group-2

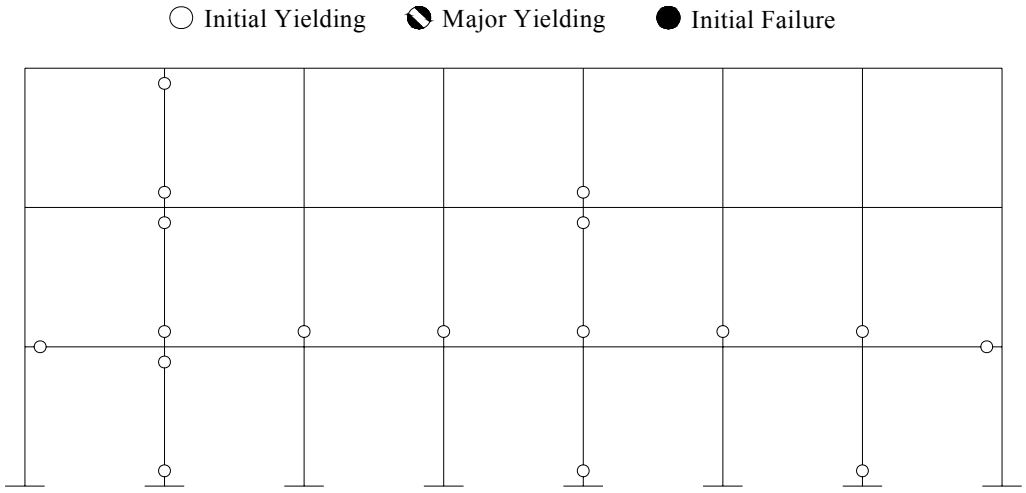

FRAME D

Figure 2.18a Hinge Patterns at Significant Yield for Group-2

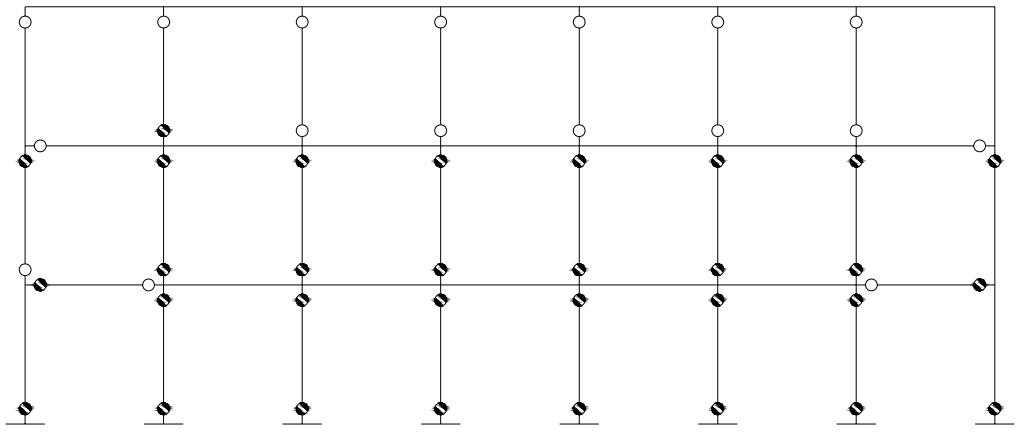

FRAME D

Figure 2.18b Hinge Patterns at the Ultimate Capacity for Group-2

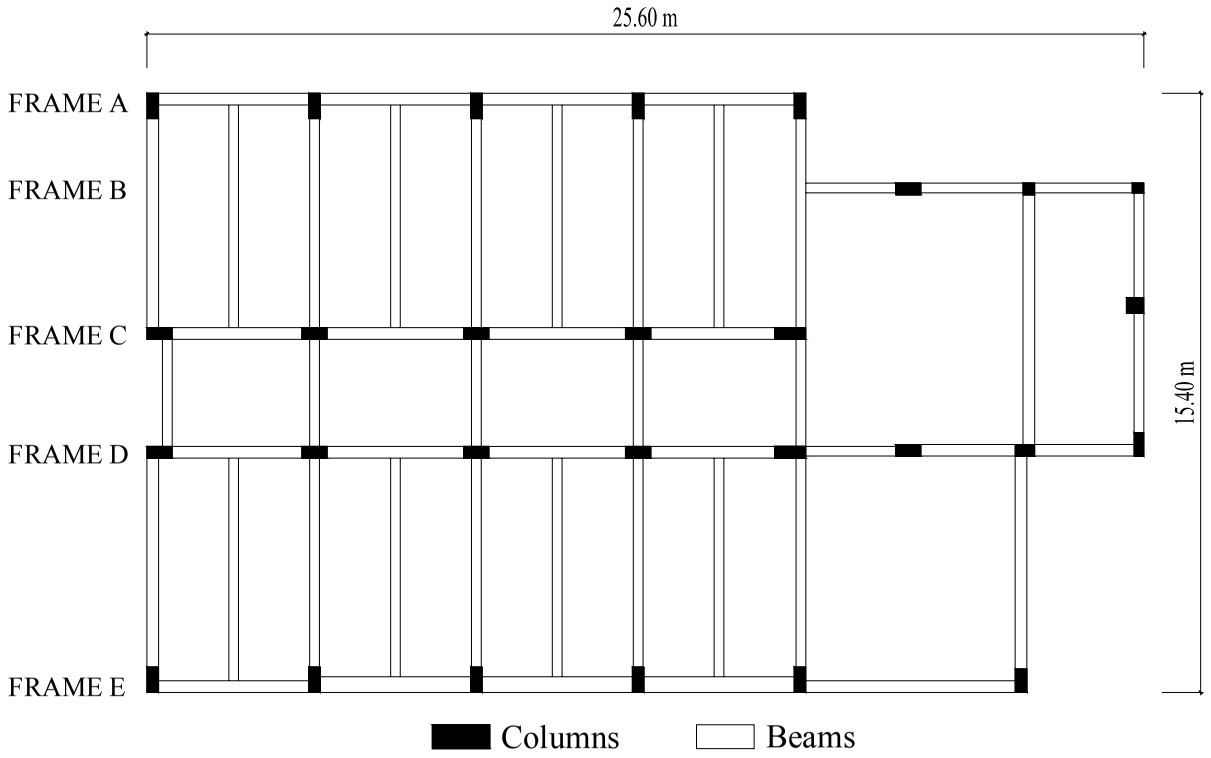

Figure 2.19 Plan Layout of the Selected Building for Group-3

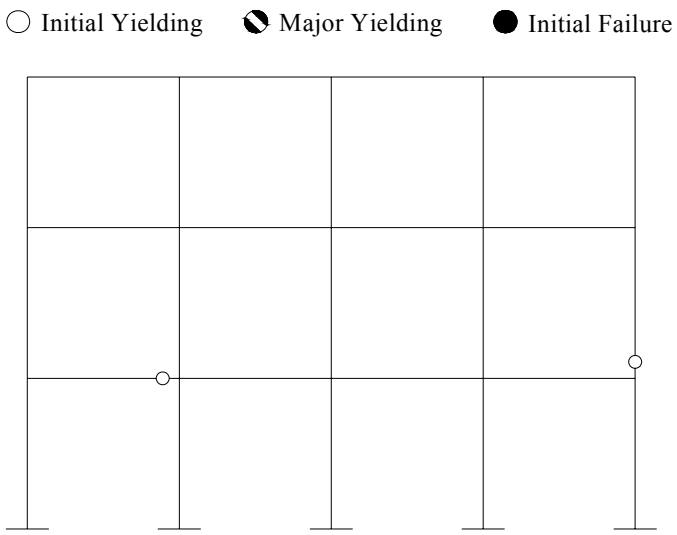

Figure 2.20a Hinge Patterns at Significant Yield for Group-3

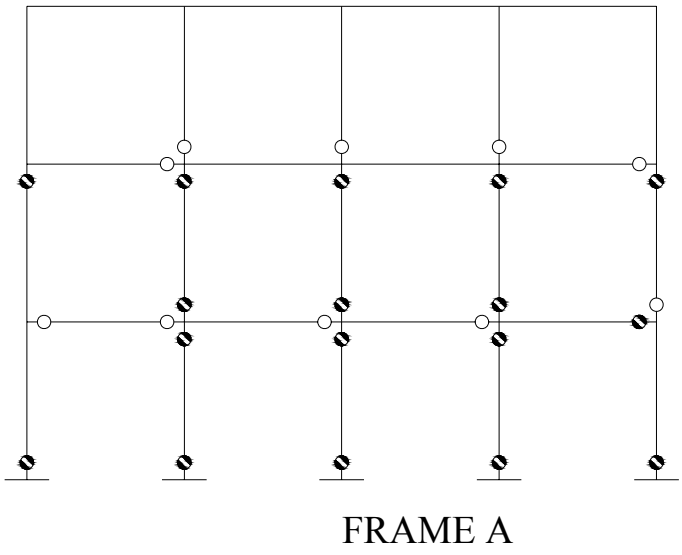

Figure 2.20b Hinge Patterns at the Ultimate Capacity for Group-3

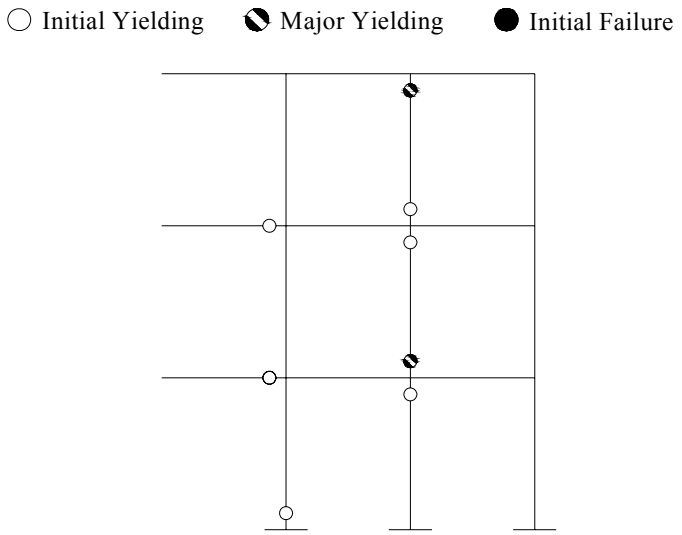

FRAME B

Figure 2.21a Hinge Patterns at Significant Yield for Group-3

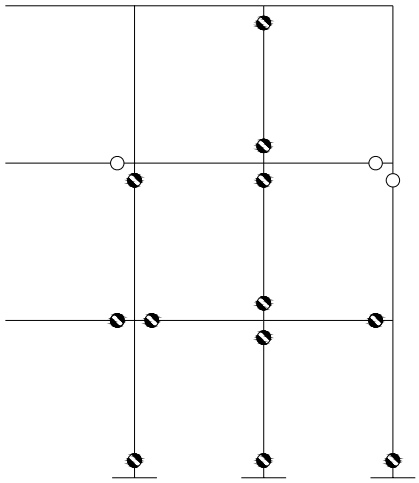

FRAME B

Figure 2.21b Hinge Patterns at the Ultimate Capacity for Group-3

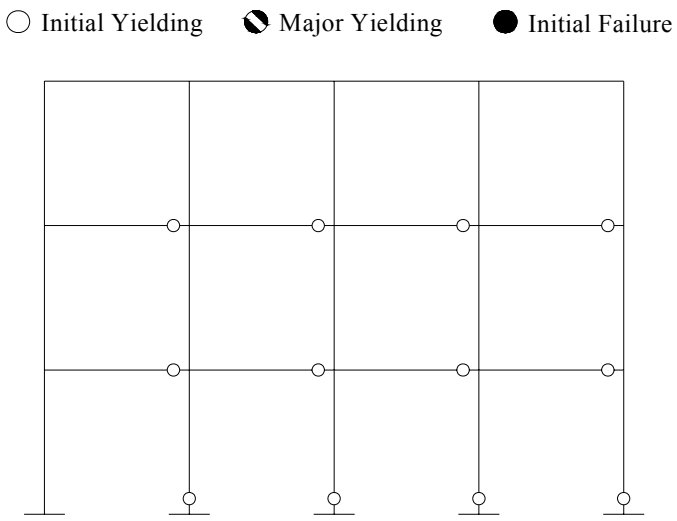

Figure 2.22a Hinge Patterns at Significant Yield for Group-3

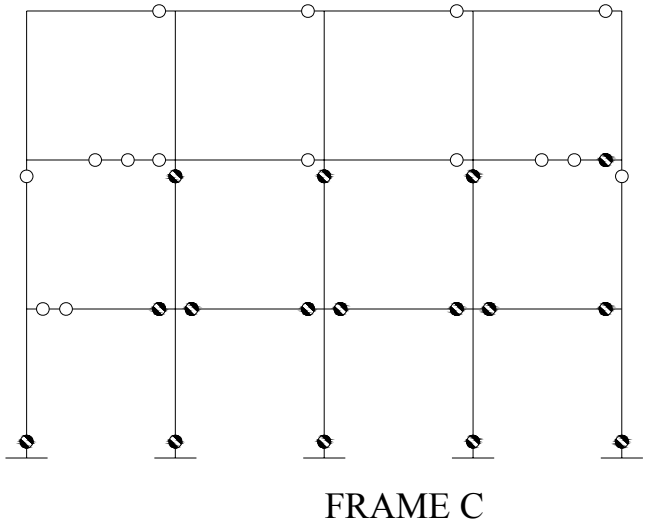

Figure 2.22b Hinge Patterns at the Ultimate Capacity for Group-3

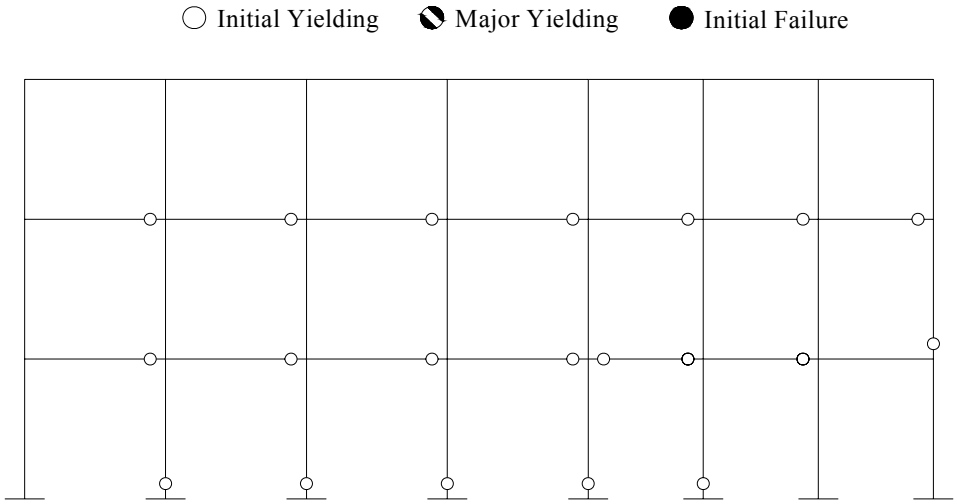

FRAME D

Figure 2.23a Hinge Patterns at Significant Yield for Group-3

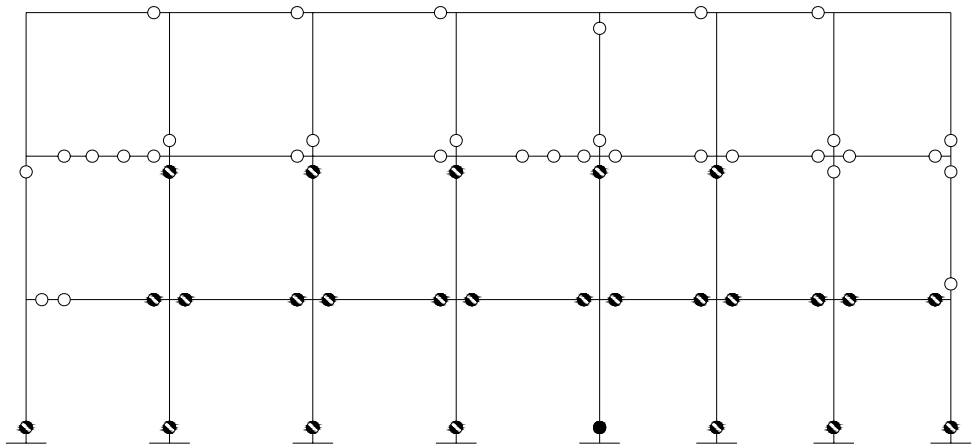

FRAME D

Figure 2.23b Hinge Patterns at the Ultimate Capacity for Group-3

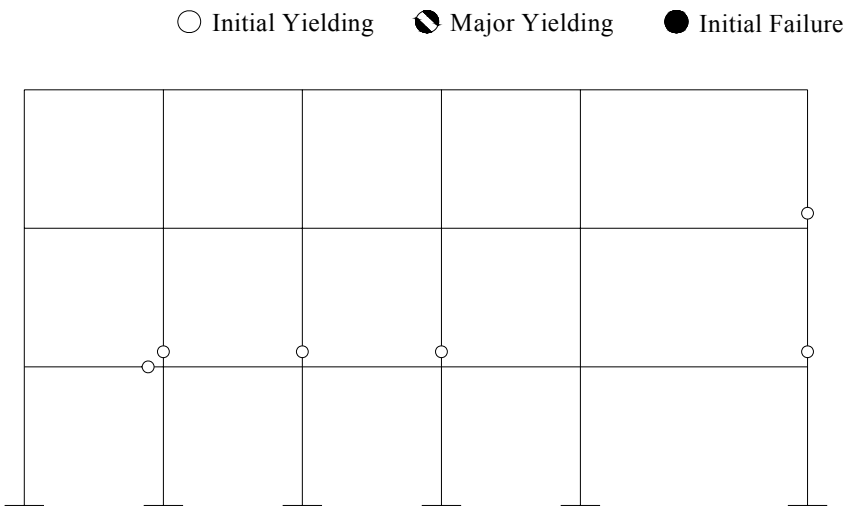

FRAME E

Figure 2.24a Hinge Patterns at Significant Yield for Group-3

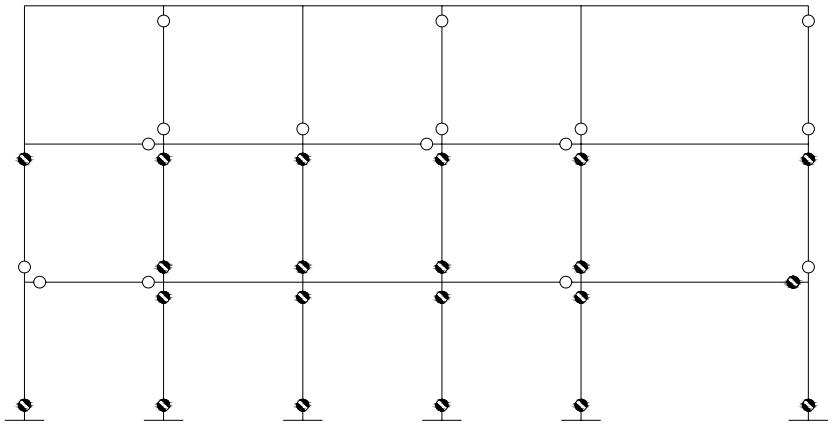

FRAME E

Figure 2.24b Hinge Patterns at the Ultimate Capacity for Group-3

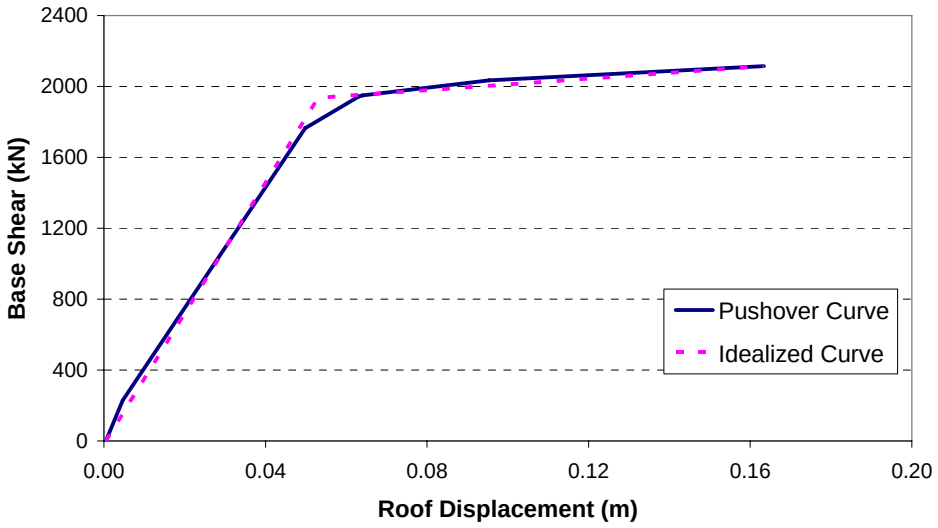

Figure 2.25 Pushover Curve of the Selected Building for Group-1

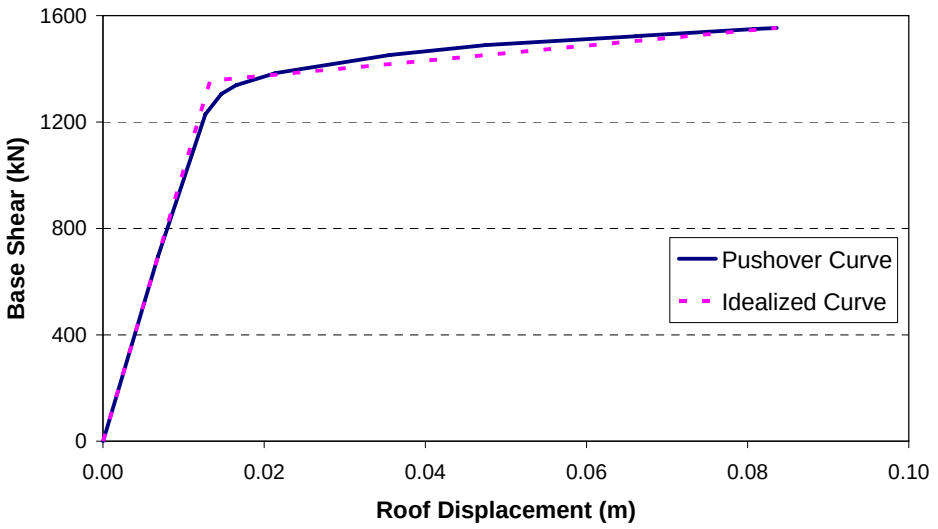

Figure 2.26 Pushover Curve of the Selected Building for Group-2

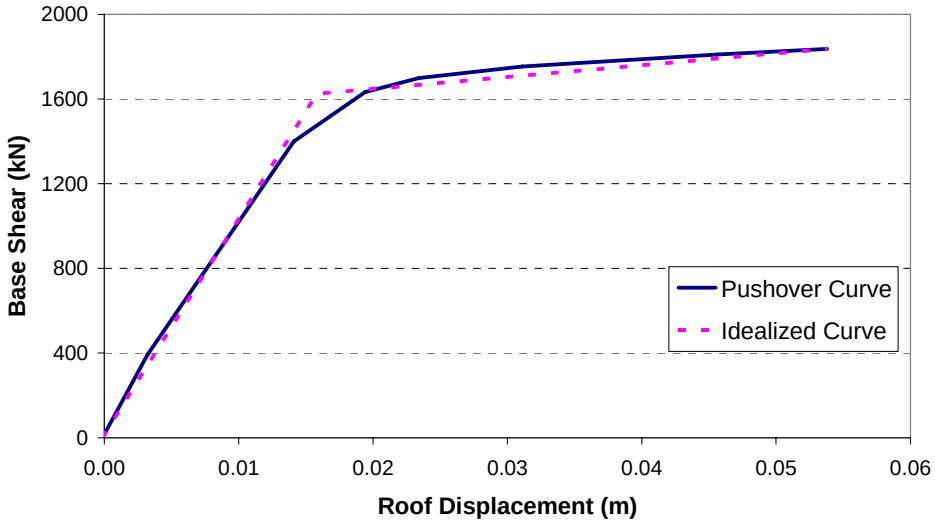

Figure 2.27 Pushover Curve of the Selected Building for Group-3

2.4 CAPACITY RELATED PROPERTIES OF THE BUILDINGS

The results of the nonlinear analyses were processed to determine parameters needed to describe the capacity curve of the typical reinforced concrete school buildings in Turkey. The statistical properties of all parameters are given in Table 2-2 for all number of stories. The statistics of capacity curve parameters for Group-1, Group-2 and Group-3 buildings are given in Table 2-3, Table 2-4 and Table 2-5, respectively. The corresponding values were calculated using Equations (1.1), (1.2), (1.3) and (1.4) for capacity curves. The capacity curve parameters for each building are given in Table A.2-1 of Appendix A.

The fundamental periods that are shown in Table 2-2 appear to be high because of the geometric properties of members and the low modulus of elasticity values (use of cracked sections). The participation factor, PF, and modal mass factor, α, for the first mode of the structure show insignificant variation with the number of stories. The yield over-strength ratios, γ, were found to decrease as number of stories increases, reaching nearly 1.0 for five story buildings. As shown in Table A.2-1 of Appendix A, the yield over-

strength ratios, γ, were found to be less than 1.0 in some cases. According to an earlier study focusing on building performance [3], reinforced concrete frame buildings that have yield over-strength ratio of less than 1.65 would perform poorly against a devastating earthquake in Turkey. The ultimate over-strength ratio, λ, for the buildings investigated ranged from 1.02-2.49. The ductility ratio, μ, was found to be low due to inappropriate detailing, irregular plans and low capacity of members.

The statistics of the properties of idealized capacity curves obtained for the school buildings are shown in Table 2-6. The approximate average drift ratios corresponding to the global yield were determined as 0.142, 0.213 and 0.264 percent for 3, 4 and 5 story buildings, respectively. Although, these drift limits are a bit higher for 4 and 5 stories than the ones obtained for residential buildings, the limits for 3 stories are close to the ones determined for residential buildings [2]. This is believed to be due to lesser degree of irregularity in school buildings compared to residential ones in Turkey. The coefficient of variation (C.O.V) was found to be large especially for 3 and 4 story buildings.

Table 2-2 Statistics of Capacity Curve Parameters

		Number of Stories		
Parameter		3	4	5
Sd_y (cm)	mean	1.14	2.36	3.56
	st. dev.	0.84	1.37	1.08
Sa_y (g)	mean	0.19	0.13	0.10
	st. dev.	0.12	0.09	0.05
Sd_u (cm)	mean	3.84	7.27	12.59
	st. dev.	3.09	4.47	2.34
Sa_u (g)	mean	0.27	0.17	0.11
	st. dev.	0.19	0.13	0.06
C_s	mean	0.09	0.07	0.07
	st. dev.	0.04	0.02	0.01
T_e	mean	0.54	0.95	1.28
	st. dev.	0.32	0.45	0.37
PF	mean	1.25	1.24	1.27
	st. dev.	0.13	0.19	0.10
α	mean	0.78	0.71	0.73
	st. dev.	0.10	0.13	0.09
γ	mean	1.83	1.39	1.06
	st. dev.	1.08	0.74	0.48
λ	mean	1.39	1.26	1.15
	st. dev.	0.30	0.26	0.08
μ	mean	2.54	2.51	3.19
	st. dev.	1.08	0.90	0.66

Table 2-3 Statistics of Capacity Curve Parameters for Group-1 Buildings

		Number of Stories		
Parameter		3	4	5
Sd_y (cm)	mean	0.14	1.99	3.08
	st. dev.	0.01	1.36	0.61
Sa_y (g)	mean	0.22	0.13	0.09
	st. dev.	0.11	0.06	0.04
Sd_u (cm)	mean	0.61	6.58	11.94
	st. dev.	0.11	4.83	2.29
Sa_u (g)	mean	0.36	0.16	0.11
	st. dev.	0.09	0.08	0.04
C_s	mean	0.05	0.07	0.07
	st. dev.	0.00	0.03	0.02
T_e	mean	0.17	0.84	1.22
	st. dev.	0.05	0.44	0.26
PF	mean	1.32	1.27	1.28
	st. dev.	0.02	0.17	0.09
α	mean	0.75	0.72	0.74
	st. dev.	0.01	0.10	0.08
γ	mean	3.42	1.51	0.99
	st. dev.	1.76	0.89	0.47
λ	mean	1.77	1.24	1.17
	st. dev.	0.50	0.17	0.08
μ	mean	2.53	2.74	3.38
	st. dev.	0.52	1.14	0.68

Table 2-4 Statistics of Capacity Curve Parameters for Group-2 Buildings

		Number of Stories		
Parameter		3	4	5
Sd_y (cm)	mean	1.23	1.88	4.98
	st. dev.	0.85	1.04	0.94
Sa_y (g)	mean	0.19	0.17	0.12
	st. dev.	0.13	0.15	0.08
Sd_u (cm)	mean	3.92	5.51	14.55
	st. dev.	2.96	3.25	1.39
Sa_u (g)	mean	0.27	0.23	0.13
	st. dev.	0.21	0.19	0.10
C_s	mean	0.10	0.08	0.06
	st. dev.	0.04	0.03	0.00
T_e	mean	0.57	0.88	1.49
	st. dev.	0.32	0.54	0.71
PF	mean	1.24	1.23	1.21
	st. dev.	0.15	0.22	0.14
α	mean	0.77	0.70	0.69
	st. dev.	0.11	0.14	0.15
γ	mean	1.51	1.32	1.24
	st. dev.	0.83	0.82	0.67
λ	mean	1.36	1.38	1.11
	st. dev.	0.24	0.40	0.09
μ	mean	2.38	2.13	2.65
	st. dev.	1.16	0.63	0.04

Table 2-5 Statistics of Capacity Curve Parameters for Group-3 Buildings

		Number of Stories		
Parameter		3	4	5
Sd_y (cm)	mean	1.57	3.62	-
	st. dev.	0.49	1.07	-
Sa_y (g)	mean	0.12	0.10	-
	st. dev.	0.02	0.05	-
Sd_u (cm)	mean	6.57	10.70	-
	st. dev.	3.38	3.56	-
Sa_u (g)	mean	0.14	0.12	-
	st. dev.	0.01	0.05	-
C_s	mean	0.05	0.05	-
	st. dev.	0.00	0.01	-
T_e	mean	0.73	1.22	-
	st. dev.	0.16	0.27	-
PF	mean	1.27	1.18	-
	st. dev.	0.03	0.21	-
α	mean	0.86	0.72	-
	st. dev.	0.05	0.16	-
γ	mean	2.18	1.28	-
	st. dev.	0.42	0.21	-
λ	mean	1.16	1.15	-
	st. dev.	0.04	0.08	-
μ	mean	3.48	2.56	-
	st. dev.	0.66	0.54	-

Table 2-6 Statistics for the Properties of Idealized Capacity Curves

Parameter	Story Number	Mean	Median	Standard Deviation	C.O.V.
Base Shear Coefficient (η)	All	0.117	0.088	0.097	0.83
	3	0.178	0.130	0.127	0.71
	4	0.090	0.079	0.064	0.71
	5	0.067	0.062	0.026	0.38
Yield Global Drift Ratio (θ_y)	All	0.00196	0.00209	0.00108	0.55
	3	0.00142	0.00127	0.00091	0.64
	4	0.00213	0.00228	0.00111	0.52
	5	0.00264	0.00251	0.00075	0.29
Ultimate Global Drift Ratio (θ_u)	All	0.00639	0.00685	0.00373	0.58
	3	0.00486	0.00424	0.00365	0.75
	4	0.00659	0.00694	0.00373	0.57
	5	0.00937	0.00906	0.00156	0.17

CHAPTER 3

ASSESSMENT OF BUILDINGS

3.1 GENERAL

As mentioned earlier, the buildings employed were assessed using the current seismic design code in effect in Turkey [33] within the ISMEP project. The buildings were also independently assessed using the displacement coefficient method and the pushover curves obtained. In order to evaluate the efficiency of existing preliminary seismic performance assessment procedures developed by Yakut [3], Hassan & Sozen [8] and Ozcebe et al. [10], these procedures were used to determine the expected seismic performance of the selected buildings. Results of the assessments based on Turkish Earthquake Code (TEC 2007) [33] and displacement coefficient method have been assumed as correct and according to these results, the correct classification rate of preliminary seismic assessment procedures was determined. The assessment results obtained from these procedures were found to be similar. The performance of the buildings is mainly grouped into three as immediate occupancy (IO), life safety (LS) and collapse prevention (CP). In addition, the physical damage states of the buildings were also identified based on the performance levels. There are mainly four damage levels that are negligible, light, moderate and heavy. The negligible and light damage states correspond to the immediate occupancy performance level. The moderate damage state corresponds to the life safety performance level and the heavy damage level corresponds to the collapse prevention.

3.2 ASSESSMENT USING EXISTING PROCEDURES

3.2.1 Yakut's Procedure [3]

The procedure developed by Yakut [3] was applied to the buildings. Capacity index (CPI) values were calculated in both x and y directions, then compared with the cut-off value. The cut-off value is assumed as 1.20. The capacity indexes, the cut-off value and performance levels of buildings are presented in Table 3-1. It is seen that performance level of 9 buildings in x direction and 15 buildings in y direction is life safety.

Table 3-1 Performance Levels of Buildings Based on Procedure Developed by Yakut [3]

	X Direction			Y Direction		
Building ID	CPI_x	Cut Off	Perf. Level	CPI_y	Cut Off	Perf. Level
BLD1	0.629	1.200	Collapse	1.257	1.200	LS
BLD2	1.459	1.200	LS	2.807	1.200	LS
BLD3	0.721	1.200	Collapse	1.621	1.200	LS
BLD4	0.516	1.200	Collapse	0.946	1.200	Collapse
BLD5	0.631	1.200	Collapse	0.579	1.200	Collapse
BLD6	0.687	1.200	Collapse	0.566	1.200	Collapse
BLD7	0.483	1.200	Collapse	0.946	1.200	Collapse
BLD8	0.440	1.200	Collapse	0.659	1.200	Collapse
BLD9	0.382	1.200	Collapse	0.765	1.200	Collapse
BLD10	0.879	1.200	Collapse	0.347	1.200	Collapse
BLD11	0.560	1.200	Collapse	1.831	1.200	LS
BLD12	0.497	1.200	Collapse	0.595	1.200	Collapse
BLD13	1.593	1.200	LS	1.659	1.200	LS
BLD14	1.324	1.200	LS	2.648	1.200	LS
BLD15	0.888	1.200	Collapse	0.678	1.200	Collapse
BLD16	0.478	1.200	Collapse	0.971	1.200	Collapse
BLD17	1.604	1.200	LS	2.013	1.200	LS

Table 3-1 (continued)

	X Direction			Y Direction		
Building ID	CPI_x	Cut Off	Perf. Level	CPI_y	Cut Off	Perf. Level
BLD18	0.684	1.200	Collapse	1.369	1.200	LS
BLD19	4.929	1.200	LS	3.483	1.200	LS
BLD20	2.725	1.200	LS	0.730	1.200	Collapse
BLD21	1.737	1.200	LS	1.618	1.200	LS
BLD22	0.630	1.200	Collapse	0.995	1.200	Collapse
BLD23	0.905	1.200	Collapse	1.817	1.200	LS
BLD24	0.850	1.200	Collapse	1.701	1.200	LS
BLD25	0.288	1.200	Collapse	0.768	1.200	Collapse
BLD26	1.459	1.200	LS	1.429	1.200	LS
BLD27	0.767	1.200	Collapse	1.535	1.200	LS
BLD28	1.082	1.200	Collapse	1.108	1.200	Collapse
BLD29	1.548	1.200	LS	1.822	1.200	LS
BLD30	0.651	1.200	Collapse	0.695	1.200	Collapse
BLD31	0.570	1.200	Collapse	0.906	1.200	Collapse
BLD32	0.464	1.200	Collapse	1.086	1.200	Collapse
BLD33	0.630	1.200	Collapse	0.630	1.200	Collapse

3.2.2 Hassan and Sozen's Procedure [8]

The procedure developed by Hassan and Sozen [8] was employed to assess the performance of the buildings. Wall index (WI) in both x and y directions and Column index (CI) values were calculated, then performances of the buildings were determined. The column index and the wall index values are presented in Figure 3-1. Performance levels of the buildings are also given in Table 3-2. It is seen that performance level of 2 buildings in x direction and 4 buildings in y direction is immediate occupancy. In addition, performance level of 14 buildings in x direction and 10 buildings in y direction is life safety.

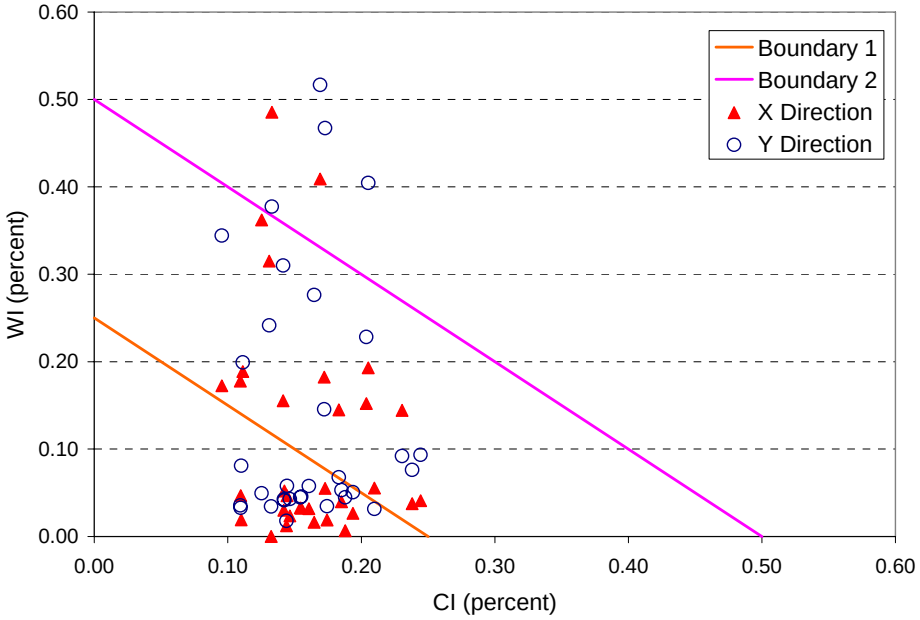

Figure 3.1 Comparison of WI and CI with the Limit Values

Table 3-2 Performance Levels of Buildings Based on Procedure Developed by Hassan and Sozen [8]

	X Direction			Y Direction		
Building ID	WI_x	CI	Perf. Level	WI_y	CI	Perf. Level
BLD1	0.1725	0.0956	LS	0.3443	0.0956	LS
BLD2	0.0398	0.1851	Collapse	0.0530	0.1851	Collapse
BLD3	0.0376	0.2381	LS	0.0762	0.2381	LS
BLD4	0.0300	0.1420	Collapse	0.0424	0.1420	Collapse
BLD5	0.0067	0.1879	Collapse	0.0449	0.1879	Collapse
BLD6	0.0123	0.1440	Collapse	0.0179	0.1440	Collapse
BLD7	0.1443	0.2305	LS	0.0920	0.2305	LS
BLD8	0.0236	0.1465	Collapse	0.0429	0.1465	Collapse
BLD9	0.0328	0.1542	Collapse	0.0448	0.1542	Collapse
BLD10	0.1779	0.1094	LS	0.0355	0.1094	Collapse
BLD11	0.0551	0.1729	Collapse	0.4672	0.1729	IO
BLD12	0.1822	0.1722	LS	0.1455	0.1722	LS
BLD13	0.1448	0.1832	LS	0.0678	0.1832	Collapse
BLD14	0.0554	0.2098	LS	0.0315	0.2098	Collapse
BLD15	0.0520	0.1424	Collapse	0.0413	0.1424	Collapse
BLD16	0.0190	0.1101	Collapse	0.0809	0.1101	Collapse

Table 3-2 (continued)

	X Direction			Y Direction		
Building ID	WI_x	CI	Perf. Level	WI_y	CI	Perf. Level
BLD17	0.1886	0.1113	LS	0.1992	0.1113	LS
BLD18	0.0000	0.1325	Collapse	0.0344	0.1325	Collapse
BLD19	0.4852	0.1330	IO	0.3773	0.1330	IO
BLD20	0.3620	0.1253	LS	0.0495	0.1253	Collapse
BLD21	0.0409	0.2444	LS	0.0934	0.2444	LS
BLD22	0.0189	0.1743	Collapse	0.0346	0.1743	Collapse
BLD23	0.1930	0.2052	LS	0.4044	0.2052	IO
BLD24	0.0266	0.1937	Collapse	0.0506	0.1937	Collapse
BLD25	0.0469	0.1096	Collapse	0.0327	0.1096	Collapse
BLD26	0.0466	0.1443	Collapse	0.0579	0.1443	Collapse
BLD27	0.0323	0.1550	Collapse	0.0457	0.1550	Collapse
BLD28	0.3150	0.1310	LS	0.2416	0.1310	LS
BLD29	0.4090	0.1692	IO	0.5167	0.1692	IO
BLD30	0.1521	0.2038	LS	0.2282	0.2038	LS
BLD31	0.1553	0.1415	LS	0.3100	0.1415	LS
BLD32	0.0163	0.1647	Collapse	0.2762	0.1647	LS
BLD33	0.0317	0.1607	Collapse	0.0576	0.1607	Collapse

3.2.3 Ozcebe et al.'s Procedure [10]

The procedure developed by Ozcebe et al. [10] was applied to the buildings. Damage index (DI) corresponding to the performance classifications and cut-off (CV) values based on number of stories for each performance classification were obtained. Then, performances of the buildings were determined by comparing the CV values with the associated DI values. The damage indexes, cut-off values and corresponding performance classification are given in Table 3-3. It is seen that performance level of 25 buildings is immediate occupancy and 8 buildings is life safety.

Table 3-3 Performance Levels of Buildings Considering Procedure Developed by Ozcebe et al. [10]

Building ID	DI_{IO}	CF_{IO}	DI_{LS}	CF_{LS}	Perf. Level
BLD1	-3.8520	-1.2783	-3.3647	0.0441	IO
BLD2	-2.0431	-0.4794	-1.2745	0.4320	IO
BLD3	-1.3938	-1.0000	-1.4746	0.0345	IO
BLD4	-0.6564	-1.0000	-0.8062	0.0345	LS
BLD5	-0.6257	-0.0016	-1.0190	0.8128	IO
BLD6	-0.4195	-0.0016	-0.0052	0.8128	IO
BLD7	-2.3455	-0.8921	-2.5285	0.8039	IO
BLD8	-0.6874	-1.0000	-1.0310	0.0345	LS
BLD9	-0.6608	-1.0000	-0.8110	0.0345	LS
BLD10	-0.7080	-0.6870	-0.8928	0.0237	IO
BLD11	-0.8916	-0.4794	-0.9131	0.4320	IO
BLD12	-2.6674	-0.6979	-2.8297	0.6289	IO
BLD13	-1.6236	-0.6979	-1.6804	0.6289	IO
BLD14	-1.2661	-0.6870	-0.7334	0.0237	IO
BLD15	-0.0347	-1.0000	-0.2071	0.0345	LS
BLD16	-0.4899	-0.0016	-0.8121	0.8128	IO
BLD17	-1.7868	-1.0000	-2.1000	0.0345	IO
BLD18	-0.6198	-0.6870	-0.8134	0.0237	LS
BLD19	-3.2385	-0.4794	-2.9295	0.4320	IO
BLD20	-0.7296	-0.6870	-0.9126	0.0237	IO
BLD21	-0.8000	-0.4794	0.0563	0.4320	IO
BLD22	-0.5403	-0.0016	-0.8948	0.8128	IO
BLD23	-5.0998	-0.6979	-4.4986	0.6289	IO
BLD24	-1.2144	-1.0000	-0.5983	0.0345	IO
BLD25	-0.6350	-1.0000	-0.7758	0.0345	LS
BLD26	-0.7297	-0.6870	-0.9249	0.0237	IO
BLD27	-0.6579	-1.0000	-0.8513	0.0345	LS
BLD28	-1.7021	-1.4701	-0.8307	0.0507	IO
BLD29	-4.5469	-0.7693	-4.7057	0.6932	IO
BLD30	-1.1499	-0.8921	-1.4121	0.8039	IO
BLD31	-2.1838	-1.2783	-2.4347	0.0441	IO
BLD32	0.0167	-1.1023	-0.3012	0.0380	LS
BLD33	-2.2217	-0.6979	-2.2371	0.6289	IO

3.3 ASSESSMENT USING DISPLACEMENT COEFFICIENT METHOD

The target displacement (Δ_d) for all buildings in both x and y directions was computed using displacement coefficient method. Then, performance limits displayed in Figure 3-2 were computed by considering yield displacement (Δ_y) and ultimate displacement (Δ_u). The ultimate displacement is accepted to be the limiting value for the collapse prevention performance level. The displacement limit for life safety performance is assigned the third quartile of the ultimate displacement. The yield displacement is accepted to be the limiting value for the immediate occupancy performance level. After that, performance levels of the buildings were determined. Yield displacement, ultimate displacement and target displacement values and performance levels of all buildings in both x and y directions are presented in Table 3-4. It is seen that the target displacements of all buildings in x direction and 31 buildings in y direction exceed the collapse prevention limit values. The performance level of the remaining two buildings in y direction is collapse prevention.

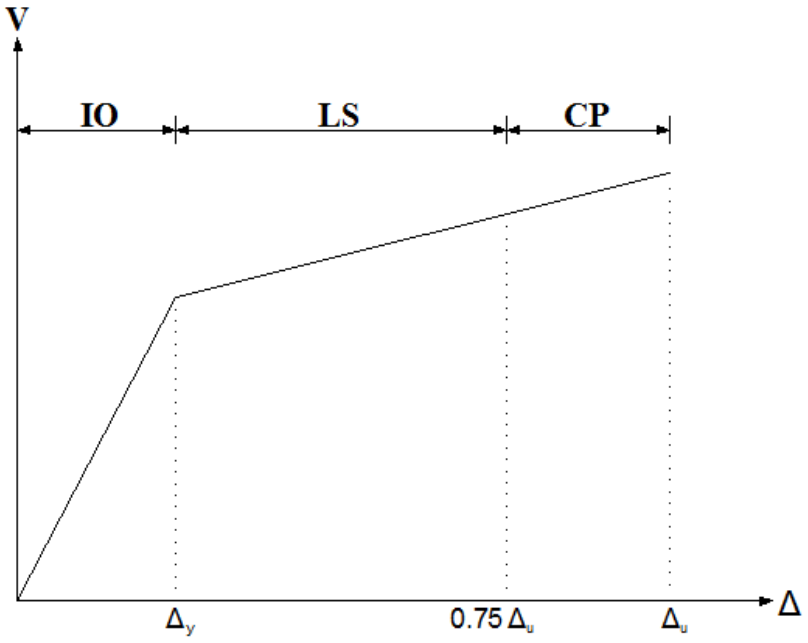

Figure 3.2 Assumed Performance Limits for Performance Levels

Table 3-4 Performance Levels of Buildings Considering Displacement Coefficient Method

	X Direction				Y Direction			
Building ID	Δ_y	Δ_u	Δ_d	Perfor. Level	Δ_y	Δ_u	Δ_d	Perfor. Level
BLD1	0.011	0.020	0.056	Collapse	0.011	0.020	0.030	Collapse
BLD2	0.037	0.105	0.190	Collapse	0.027	0.101	0.114	Collapse
BLD3	0.024	0.093	0.137	Collapse	0.030	0.070	0.157	Collapse
BLD4	0.027	0.065	0.224	Collapse	0.025	0.065	0.224	Collapse
BLD5	0.033	0.127	0.296	Collapse	0.045	0.173	0.320	Collapse
BLD6	0.046	0.156	0.308	Collapse	0.044	0.169	0.302	Collapse
BLD7	0.013	0.084	0.253	Collapse	0.020	0.055	0.308	Collapse
BLD8	0.040	0.104	0.313	Collapse	0.036	0.121	0.288	Collapse
BLD9	0.053	0.163	0.381	Collapse	0.045	0.180	0.395	Collapse
BLD10	0.008	0.023	0.089	Collapse	0.052	0.155	0.217	Collapse
BLD11	0.017	0.046	0.086	Collapse	0.005	0.016	0.014	CP
BLD12	0.007	0.019	0.095	Collapse	0.013	0.022	0.143	Collapse
BLD13	0.006	0.017	0.276	Collapse	0.027	0.097	0.131	Collapse
BLD14	0.045	0.144	0.237	Collapse	0.045	0.134	0.172	Collapse
BLD15	0.020	0.043	0.151	Collapse	0.036	0.111	0.175	Collapse
BLD16	0.074	0.204	0.431	Collapse	0.048	0.151	0.193	Collapse
BLD17	0.008	0.040	0.136	Collapse	0.006	0.013	0.099	Collapse
BLD18	0.053	0.146	0.249	Collapse	0.046	0.120	0.214	Collapse
BLD19	0.002	0.007	0.020	Collapse	0.002	0.009	0.097	Collapse
BLD20	0.006	0.021	0.073	Collapse	0.039	0.097	0.126	Collapse
BLD21	0.016	0.054	0.088	Collapse	0.024	0.112	0.118	Collapse
BLD22	0.035	0.169	0.229	Collapse	0.033	0.121	0.154	Collapse
BLD23	0.006	0.012	0.046	Collapse	0.004	0.010	0.032	Collapse
BLD24	0.029	0.116	0.196	Collapse	0.029	0.074	0.167	Collapse
BLD25	0.031	0.089	0.379	Collapse	0.029	0.080	0.266	Collapse
BLD26	0.012	0.055	0.074	Collapse	0.022	0.147	0.110	CP
BLD27	0.039	0.152	0.246	Collapse	0.048	0.125	0.208	Collapse
BLD28	0.006	0.015	0.112	Collapse	0.007	0.017	0.122	Collapse
BLD29	0.010	0.032	0.268	Collapse	0.010	0.024	0.120	Collapse
BLD30	0.020	0.104	0.542	Collapse	0.023	0.059	0.491	Collapse
BLD31	0.029	0.090	0.205	Collapse	0.029	0.090	0.173	Collapse
BLD32	0.028	0.087	0.349	Collapse	0.028	0.087	0.333	Collapse
BLD33	0.015	0.053	0.146	Collapse	0.015	0.053	0.142	Collapse

3.4 COMPARISONS AND INTERPRETATION

The results that are obtained from all assessment methods considered are summarized in Tables 3-5 and 3-6 in x- and y-directions, respectively. These tables also present the final decision regarding the action to be taken. According to the assessment reports for the school buildings prepared by PROMER Consultancy Engineering Ltd. Co. in consultancy with Middle East Technical University (METU), none of the buildings fully satisfy the requirements of the Turkish code [33]. The decision regarding the action to be taken for the rehabilitation of the buildings (whether to retrofit or demolish) was made based on both requirements of the Turkish Earthquake Code and cost of the action. If the ratio of retrofitting cost to reconstruction cost exceeded 40 percent, it was decided to suggest demolishing the existing building. Otherwise, the buildings were retrofitted. The last column in Tables 3-5 and 3-6 indicate the basis of the decision taken. The displacement coefficient method determines the performance level of almost all buildings as collapse. According to Ozcebe et al.'s procedure [10], performance levels of 25 buildings are Immediate Occupancy whereas Yakut's procedure [3] determines the performance level of 24 buildings in x direction and 18 buildings in y direction as collapse. This indicates that the classification of Ozcebe et al.'s procedure [10] is generally not in compliance with other procedures. This is believed to be due to parameters involved in this procedure. Ozcebe et al.'s procedure [10] is based on the statistical assessment of observed damage using mostly architectural attributes such as overhangs, soft story, number of stories etc. The school buildings generally do not possess many of these architectural features which are quite dominant in Ozcebe et al.'s procedure [10]. Other procedures, however, rely mostly on the capacity of structural members. In Hassan and Sozen's procedure [8], the correct classification rate of buildings is approximately 55 percent. This difference can be explained by that the procedure developed by Yakut [3] considers strength of concrete, regional seismicity, the negative effect of architectural features and the quality of

construction in addition to the dimensions of the structure. Moreover, soft story, short column, in-plan and vertical irregularity are also taken into account whereas the procedure developed by Hassan & Sozen [8] requires only the total floor area and cross-sectional areas of columns, shear walls and masonry walls of structure.

For the sake of completeness the buildings were also assessed according to the global drift limits given in ATC-40 [30]. The global drift ratio values were determined as ratio of target displacement calculated using displacement coefficient method to building height. The results of performance classification are also shown in Table 3-5 and Table 3-6. The reason for the results that are generally not in agreement with other procedures is that the drift limits given in ATC-40 [30] are very unconservative for Turkish buildings since they are recommended for US buildings that are expected to be in good compliance with the codes.

Table 3-5 Comparison of the Results of Procedures in X Direction

Building ID	Dis. Coef. Method	TEC 2007	ATC-40	Yakut	Hassan& Sozen	Ozcebe et al.	Decision	Explanation
BLD1	Collapse	Inadequate	IO	Collapse	LS	IO	Retrofitting	due to TEC 2007
BLD2	Collapse	Inadequate	LS	LS	Collapse	IO	Demolishing	due to uneconomical
BLD3	Collapse	Inadequate	LS	Collapse	LS	IO	Retrofitting	due to TEC 2007
BLD4	Collapse	Inadequate	LS	Collapse	Collapse	LS	Retrofitting	due to TEC 2007
BLD5	Collapse	Inadequate	LS	Collapse	Collapse	IO	Retrofitting	due to TEC 2007
BLD6	Collapse	Inadequate	LS	Collapse	Collapse	IO	Retrofitting	due to TEC 2007
BLD7	Collapse	Inadequate	Collapse	Collapse	LS	IO	Demolishing	due to uneconomical and TEC 2007
BLD8	Collapse	Inadequate	Collapse	Collapse	Collapse	LS	Retrofitting	due to TEC 2007
BLD9	Collapse	Inadequate	Collapse	Collapse	Collapse	LS	Retrofitting	due to TEC 2007
BLD10	Collapse	Inadequate	IO	Collapse	LS	IO	Retrofitting	due to TEC 2007
BLD11	Collapse	Inadequate	LS	Collapse	Collapse	IO	Retrofitting	due to TEC 2007
BLD12	Collapse	Inadequate	IO	Collapse	LS	IO	Demolishing	due to uneconomical and TEC 2007
BLD13	Collapse	Inadequate	Collapse	LS	LS	IO	Retrofitting	due to TEC 2007
BLD14	Collapse	Inadequate	LS	LS	LS	IO	Retrofitting	due to TEC 2007
BLD15	Collapse	Inadequate	LS	Collapse	Collapse	LS	Retrofitting	due to TEC 2007
BLD16	Collapse	Inadequate	Collapse	Collapse	Collapse	IO	Retrofitting	due to TEC 2007

Table 3-5 (continued)

Building ID	Dis. Coef. Method	TEC 2007	ATC-40	Yakut	Hassan& Sozen	Ozcebe et al.	Decision	Explanation
BLD17	Collapse	Inadequate	LS	LS	LS	IO	Retrofitting	due to TEC 2007
BLD18	Collapse	Inadequate	LS	Collapse	Collapse	LS	Retrofitting	due to TEC 2007
BLD19	Collapse	Inadequate	IO	LS	IO	IO	Retrofitting	due to TEC 2007
BLD20	Collapse	Inadequate	IO	LS	LS	IO	Retrofitting	due to TEC 2007
BLD21	Collapse	Inadequate	IO	LS	LS	IO	Retrofitting	due to TEC 2007
BLD22	Collapse	Inadequate	LS	Collapse	Collapse	IO	Retrofitting	due to TEC 2007
BLD23	Collapse	Inadequate	IO	Collapse	LS	IO	Retrofitting	due to TEC 2007
BLD24	Collapse	Inadequate	LS	Collapse	Collapse	IO	Retrofitting	due to TEC 2007
BLD25	Collapse	Inadequate	Collapse	Collapse	Collapse	LS	Retrofitting	due to TEC 2007
BLD26	Collapse	Inadequate	IO	LS	Collapse	IO	Retrofitting	due to TEC 2007
BLD27	Collapse	Inadequate	LS	Collapse	Collapse	LS	Demolishing	due to uneconomical
BLD28	Collapse	Inadequate	IO	Collapse	LS	IO	Demolishing	due to uneconomical and TEC 2007
BLD29	Collapse	Inadequate	Collapse	LS	IO	IO	Retrofitting	due to TEC 2007
BLD30	Collapse	Inadequate	Collapse	Collapse	LS	IO	Retrofitting	due to TEC 2007
BLD31	Collapse	Inadequate	LS	Collapse	LS	IO	Retrofitting	due to TEC 2007
BLD32	Collapse	Inadequate	Collapse	Collapse	Collapse	LS	Retrofitting	due to TEC 2007
BLD33	Collapse	Inadequate	LS	Collapse	Collapse	IO	Retrofitting	due to TEC 2007

Table 3-6 Comparison of the Results of Procedures in Y Direction

Building ID	Dis. Coef. Method	TEC 2007	ATC-40	Yakut	Hassan& Sozen	Ozcebe et al.	Decision	Explanation
BLD1	Collapse	Inadequate	IO	LS	LS	IO	Retrofitting	due to TEC 2007
BLD2	Collapse	Inadequate	IO	LS	Collapse	IO	Demolishing	due to uneconomical
BLD3	Collapse	Inadequate	LS	LS	LS	IO	Retrofitting	due to TEC 2007
BLD4	Collapse	Inadequate	LS	Collapse	Collapse	LS	Retrofitting	due to TEC 2007
BLD5	Collapse	Inadequate	Collapse	Collapse	Collapse	IO	Retrofitting	due to TEC 2007
BLD6	Collapse	Inadequate	LS	Collapse	Collapse	IO	Retrofitting	due to TEC 2007
BLD7	Collapse	Inadequate	Collapse	Collapse	LS	IO	Demolishing	due to uneconomical and TEC 2007
BLD8	Collapse	Inadequate	Collapse	Collapse	Collapse	LS	Retrofitting	due to TEC 2007
BLD9	Collapse	Inadequate	Collapse	Collapse	Collapse	LS	Retrofitting	due to TEC 2007
BLD10	Collapse	Inadequate	LS	Collapse	Collapse	IO	Retrofitting	due to TEC 2007
BLD11	CP	Inadequate	IO	LS	IO	IO	Retrofitting	due to TEC 2007
BLD12	Collapse	Inadequate	LS	Collapse	LS	IO	Demolishing	due to uneconomical and TEC 2007
BLD13	Collapse	Inadequate	LS	LS	Collapse	IO	Retrofitting	due to TEC 2007
BLD14	Collapse	Inadequate	LS	LS	Collapse	IO	Retrofitting	due to TEC 2007
BLD15	Collapse	Inadequate	LS	Collapse	Collapse	LS	Retrofitting	due to TEC 2007
BLD16	Collapse	Inadequate	LS	Collapse	Collapse	IO	Retrofitting	due to TEC 2007

Table 3-6 (continued)

Building ID	Dis. Coef. Method	TEC 2007	ATC-40	Yakut	Hassan& Sozen	Ozcebe et al.	Decision	Explanation
BLD17	Collapse	Inadequate	IO	LS	LS	IO	Retrofitting	due to TEC 2007
BLD18	Collapse	Inadequate	LS	LS	Collapse	LS	Retrofitting	due to TEC 2007
BLD19	Collapse	Inadequate	LS	LS	IO	IO	Retrofitting	due to TEC 2007
BLD20	Collapse	Inadequate	LS	Collapse	Collapse	IO	Retrofitting	due to TEC 2007
BLD21	Collapse	Inadequate	LS	LS	LS	IO	Retrofitting	due to TEC 2007
BLD22	Collapse	Inadequate	IO	Collapse	Collapse	IO	Retrofitting	due to TEC 2007
BLD23	Collapse	Inadequate	IO	LS	IO	IO	Retrofitting	due to TEC 2007
BLD24	Collapse	Inadequate	LS	LS	Collapse	IO	Retrofitting	due to TEC 2007
BLD25	Collapse	Inadequate	LS	Collapse	Collapse	LS	Retrofitting	due to TEC 2007
BLD26	CP	Inadequate	IO	LS	Collapse	IO	Retrofitting	due to TEC 2007
BLD27	Collapse	Inadequate	LS	LS	Collapse	LS	Demolishing	due to uneconomical
BLD28	Collapse	Inadequate	IO	Collapse	LS	IO	Demolishing	due to uneconomical and TEC 2007
BLD29	Collapse	Inadequate	LS	LS	IO	IO	Retrofitting	due to TEC 2007
BLD30	Collapse	Inadequate	Collapse	Collapse	LS	IO	Retrofitting	due to TEC 2007
BLD31	Collapse	Inadequate	LS	Collapse	LS	IO	Retrofitting	due to TEC 2007
BLD32	Collapse	Inadequate	Collapse	Collapse	LS	LS	Retrofitting	due to TEC 2007
BLD33	Collapse	Inadequate	LS	Collapse	Collapse	IO	Retrofitting	due to TEC 2007

CHAPTER 4

CONCLUSIONS AND RECOMMENDATIONS

4.1 SUMMARY AND CONCLUSIONS

In this study, it is aimed to determine capacity related properties of school buildings and to investigate the applicability of existing seismic vulnerability assessment procedures on school buildings in Turkey. Thirty three reinforced concrete school buildings were extracted from the ISMEP project. The average value of compressive concrete strength of school buildings was approximately 12 MPa. All buildings unsatisfy the requirements of the Turkish code [33]. Nonlinear static analysis was conducted to obtain pushover curves from which the capacity related properties of school buildings were determined.

The following conclusions were drawn;

- The capacity curve parameters determined are believed to represent properties of typical school buildings in Turkey. These properties can be used to assess approximately the seismic performance as well as loss estimation of existing school buildings.
- The yield over-strength ratios, γ, were found to decrease as number of stories increases, reaching nearly 1.0 for five story buildings.
- The ultimate over-strength ratio, λ, for the buildings investigated ranged from 1.02 - 2.49. Because of inappropriate detailing, irregular plans and low capacity of members, the ductility ratio, μ, was found to be low.
- The mean yield base shear coefficients were determined as 0.19, 0.13 and 0.10 for 3, 4 and 5 stories, respectively. These

capacities that are similar to the ones obtained for residential buildings indicate that most of the existing school buildings have quite low seismic capacity.

- The results showed that the buildings experienced three different mechanisms as inferred from the formation and progress of hinges; beam mechanism, column mechanism and mixed mechanism.
- Existing procedures developed by Yakut [3], Hassan & Sozen [8] and Ozcebe et al. [10] and displacement coefficient method were carried out to evaluate the applicability of the existing procedures. Although none of the procedures were found to adequately determine the performance, the procedure developed by Yakut [3] is the most suitable one to assess approximately the performance of existing reinforced concrete school buildings.

4.2 RECOMMENDATIONS FOR FUTURE STUDIES

It is clear that extension of the study to include more building configurations will lead to more reliable results. A specific preliminary assessment procedure for school buildings should be developed based on more comprehensive analyses. The study can also be extended to develop fragility curves for school buildings in Turkey.

REFERENCES

[1] Yakut A. (2008). "*Capacity Related Properties of RC Frame Buildings in Turkey"*, Journal of Earthquake Engineering, Vol. 12, pp. 1–8.

[2] Akkar S., Sucuoglu H., and Yakut A., (2005). "*Displacement-Based Fragility Functions for Low- and Mid-rise Ordinary Concrete Buildings"*, Earthquake Spectra, Vol. 21, No. 4, pp. 901–927.

[3] Yakut A. (2004). "*Preliminary Seismic Performance Assessment Procedure for Existing RC Buildings"*, Engineering Structures, Vol. 26, No. 10, pp. 1447–1462.

[4] Yakut A., Tonguc Y., and Gulkan P., (2008). "*A Comparative Seismic Performance Assessment and Rehabilitation of Existing School Buildings"*, The 14th World Conference on Earthquake Engineering, Beijing, China.

[5] Erduran, E. (2005) "*Component Based Seismic Vulnerability Assessment Procedure for RC Buildings"*, Turkey, Ph.D. Thesis, Middle East Technical University, Ankara.

[6] HAZUS (1997) "*Earthquake Loss Estimation Methodology"*, Vol. I, National Institute of Building Sciences.

[7] Kircher, C.A., Whitman, R.V., and Holmes, W.T. (2006) "*HAZUS Earthquake Loss Estimation Methodology"*, Natural Hazards Review, Vol. 7, No. 2.

[8] Hassan, A.F., and Sozen, M.A., (1997) "*Seismic Vulnerability Assessment of Low-Rise Buildings in Regions with Infrequent Earthquakes"*, ACI Structural Journal, Vol. 94, No. 1.

[9] Yakut A. (2004) "*A Preliminary Seismic Assessment Procedure for Reinforced Concrete Buildings in Turkey"*, 13th World Conference on Earthquake Engineering, Vancouver, B.C., Canada, Paper No.897.

[10] Ozcebe, G., Yucemen, M.S., Yakut, A., and Aydogan, V., (2003) "*Seismic Vulnerability Assessment Procedure for Low- to Medium-Rise Reinforced Concrete Buildings"*, Turkey, Structural Engineering Research Unit, Middle East Technical University, Ankara.

[11] Ozcebe, G., Sucuoglu, H., Yucemen, M.S., Yakut, A., and Kubin, J., "*Seismic Risk Assessment of Existing Building Stock in Istanbul-A Pilot Application in Zeytinburnu District"*, Turkey, Middle East Technical University, Ankara.

[12] Yakut, A., (2006) "*Yapıların Sismik Performans Değerlendirme Yöntemleri ve Yapıların TDY 2006'ya Göre Değerlendirilmesi"*, Kurs Notları.

[13] Federal Emergency Management Agency (FEMA), "*Improvement of Nonlinear Static Seismic Analysis Procedures"*, FEMA-440.

[14] Turer, A., Akyuz, U., Yakut, A., and Yalim, B., (2003) "*School Building Damage Assessment after Bingöl Earthquake*", International Conference in Earthquake Engineering to Mark 40 Years from Catastrophic 1963, Skopje, CD-ROM.

[15] Turel, G., Pay, A.C., Ramirez, A.J., Sozen, M.A., Johnson, A.M., Irfanoglu, A., and Bobet, A., (2009) "*Performance of School Buildings in Turkey During the 1999 Düzce and the 2003 Bingöl Earthquakes"*, Earthquake Spectra, Vol. 25, No:2, pp. 239–256.

[16] Gulkan, P., (2004) "*Seismic Safety of School Buildings in Turkey: Obstacles Impeding the Achievable?*", OECD Programme on Educational Building (PEB) and Geohazards International (GHI) OECD Headquarters, Paris, 9-11 February.

[17] Gulkan, P., and Sozen, M., (1999) "*Procedure for Determining Seismic Vulnerability of Building Structures*", ACI Structural Journal, Vol. 96, No. 3.

[18] Gulkan, P., and Utkutug, D., (2003) "*Okul Binalarının Deprem Güvenliği İçin Minimum Dizayn Kriterleri*", Türkiye Mühendislik Haberleri, Sayı 425-3.

[19] Bilgin, H., Kaplan, H., and Yilmaz, S., (2008) "*Seismic Assessment of Existing R.C. Public Buildings in Turkey – An Overview with a Case Study*", Intersections/Intersectii, Vol. 5, No. 3.

[20] Elgin, K.G., (2007) "*Istanbul Seismic Risk Mitigation and Emergency Preparedness Project (ISMEP)*", Turkey, International Earthquake Symposium, Kocaeli.

[21] Dogangun, A., (2004) "*Performance of Reinforced Concrete Buildings During the May 1, 2003 Bingöl Earthquake in Turkey*", Engineering Structures, Vol. 26, pp. 841–856.

[22] Japan International Co-operation Agency and Istanbul Metropolitan Municipality (2002) "*The Study on a Disaster Prevention / Mitigation Basic Plan in Istanbul Including Seismic Microzonation in the Republic of Turkey*", Final Report, Tokyo-Istanbul.

[23] Bogazici University, Department of Earthquake Engineering (2002) "*Earthquake Risk Assessment for Istanbul Metropolitan Area*", Final Report, Kandilli Observatory and Earthquake Research Center.

[24] Krawinkler, H. and Seneviratna, G.D.P.K., 1998, "*Pros and Cons of a Pushover Analysis of Seismic Performance Evaluation*", Engineering Structures, Vol.20, pp. 452–464.

[25] Oguz, S. (2005) "*Evaluation of Pushover Analysis Procedures for Frame Structures*" Turkey, M.S. Thesis, Middle East Technical University, Ankara.

[26] Duzce, Z. (2006) "*Performance Evaluation of Existing Medium Rise Reinforced Concrete Buildings According to 2006 Turkish Seismic Rehabilitation Code*" Turkey, M.S. Thesis, Middle East Technical University, Ankara.

[27] Yakut, A., Yucemen, M.S., and Ozcebe, G., (2006) "*Seismic Vulnerability Assessment Using Regional Empirical Data"*, Earthquake Engineering and Structural Dynamics, Vol. 35, pp. 1187–1202.

[28] Ozcebe, G., Yucemen, M.S., Aydogan, V., and Yakut, A., "*Preliminary Seismic Vulnerability Assessment of Reinforced Concrete Buildings in Turkey-Part I: Statistical Model Based on Structural Characteristics"*, Seismic Assessment and Rehabilitation of Existing Buildings, NATO Science Series, Vol IV/29, Kluwer Academic Publishers, Netherlands, Nov. 2003, pp. 29-42.

[29] Yakut, A., Aydogan, V., Ozcebe, G., and Yucemen, M.S., "*Preliminary Seismic Vulnerability Assessment of Reinforced Concrete Buildings in Turkey-Part II: Inclusion of Site Characteristics"*, Seismic Assessment and Rehabilitation of Existing Buildings, NATO Science Series, Vol IV/29, Kluwer Academic Publishers, Netherlands, Nov. 2003, pp. 43-58.

[30] ATC-40 (1996), "*Seismic Evaluation and Retrofit of Concrete Buildings"*, Applied Technology Council.

[31] FEMA-356 (2000) "*Prestandard and Commentary for the Seismic Rehabilitation of Buildings*", American Society of Civil Engineers, FEMA, Washington, D.C.

[32] Computer and Structures Inc. (CSI), (1998) "*SAP2000 Three Dimensional Static and Dynamic Finite Element Analysis and Design of Structure V7.40",* Berkeley, California.

[33] Turkish Earthquake Code (2007) "*Specifications for the Buildings to be Constructed in Disaster Areas",* Ministry of Public Works and Settlement, Ankara, Turkey.

[34] "*March 13, 1992 (Ms=6.8), Erzincan Earthquake: A Preliminary Reconnaissance Report",* Kandilli Observatory and Earthquake Research Institute and Faculty of Engineering, Department of Civil Engineering, Bogazici University, May 1992, 119 p.

[35] Kircher, C.A., Nassar, A.A., Kustu, O. and Holmes, W.T. (1997) "*Development of Building Damage Functions for Earthquake Loss Estimation"*, Earthquake Spectra, Vol. 13, No. 4.

APPENDIX A

PROPERTIES OF BUILDINGS AND RESULTS OF ANALYSIS

A.1 DETAILED PROPERTIES OF SELECTED BUILDINGS

Detailed properties of all selected buildings are summarized in Table A.1-1 and A.1-2.

Table A.1-1 General Properties of Selected Buildings

Building ID	Construction Date	Story Number	Floor Area (m^2)	Total Building Area (m^2)	T_x (s)	T_y (s)	Soil Group & Local Site Class	EQ Region	f_{ck} (Mpa)	f_{ctk} (Mpa)
BLD1	1983	4	595	2380	0.292	0.218	C-Z3	2	9.70	1.09
BLD2	1966	3	435	1305	1.189	0.813	A-Z1	2	16.00	1.59
BLD3	1964	4	335	1340	0.684	0.608	B-Z2	2	11.20	1.17
BLD4	1965	4	655	2620	1.233	1.082	C-Z2	2	10.80	1.15
BLD5	1970	5	356	1780	0.849	1.023	C-Z2	1	13.60	1.29
BLD6	1970	5	653	3265	1.278	1.380	C-Z2	2	12.00	1.21
BLD7	1984	3	315	945	0.522	0.462	D-Z3	1	10.70	1.14
BLD8	1964	4	475	1900	1.208	0.914	C-Z2	1	13.20	1.27
BLD9	1960	4	540	2160	1.064	1.277	C-Z2	1	10.50	1.13
BLD10	1995	4	425	1700	0.445	1.067	B-Z1	2	14.70	1.34
BLD11	1976	3	320	960	0.531	0.146	A-Z1	2	12.00	1.21
BLD12	1987	3	780	2340	0.360	0.764	B-Z2	2	8.80	0.74
BLD13	1965	3	630	1890	0.336	0.686	C-Z2	2	18.20	1.49
BLD14	1964	4	410	1640	1.457	0.814	A-Z1	2	14.00	1.31
BLD15	1964	4	650	2600	0.791	1.000	B-Z2	2	12.80	1.25
BLD16	1964	5	505	2525	1.770	0.847	B-Z2	2	16.50	1.42

Table A.1-1 (continued)

Building ID	Construction Date	Story Number	Floor Area (m^2)	Total Building Area (m^2)	T_x (s)	T_y (s)	Soil Group & Local Site Class	EQ Region	f_{ck} (Mpa)	f_{ctk} (Mpa)
BLD17	1956	4	700	2800	0.466	0.459	C-Z2	2	17.70	1.47
BLD18	1960	4	545	2180	1.277	1.245	B-Z1	2	13.30	1.28
BLD19	1972	3	322	966	0.133	0.217	B-Z1	2	7.10	1.24
BLD20	1973	4	520	2080	0.278	0.833	B-Z1	2	8.00	0.99
BLD21	1973	3	355	1065	0.565	0.757	B-Z1	2	8.50	1.02
BLD22	1964	5	495	2475	1.100	0.728	B-Z2	2	11.20	1.17
BLD23	1984	3	430	1290	0.218	0.160	C-Z2	2	9.60	1.08
BLD24	1973	4	555	2220	1.039	0.841	C-Z2	2	9.80	1.10
BLD25	1973	4	413	1652	1.763	1.288	C-Z2	2	9.50	1.24
BLD26	1972	4	425	1700	0.439	0.631	B-Z1	2	12.80	1.25
BLD27	1972	4	625	2500	1.267	0.800	B-Z2	2	14.20	1.32
BLD28	1973	4	310	1240	0.338	0.367	B-Z2	2	7.00	0.70
BLD29	1990	3	260	780	0.276	0.195	B-Z4	2	10.40	1.13
BLD30	1990	3	355	1065	0.456	0.232	B-Z3	1	9.30	1.07
BLD31	1990	4	800	3200	0.596	0.512	B-Z4	2	8.30	1.01
BLD32	1990	4	800	3200	0.336	0.234	B-Z3	1	12.30	1.23
BLD33	1995	3	560	1680	0.846	0.825	B-Z2	2	7.00	0.93

Table A.1-2 Cross-Sectional Area of Columns and Walls at Base

	X DIRECTION				Y DIRECTION				
Building ID	ΣA_{Column} (m^2)	$\Sigma A_{Shear\ Wall}$ (m^2)	$\Sigma A_{Masonry\ Wall}$ (m^2)	Shear Wall Density (percent)	ΣA_{Column} (m^2)	$\Sigma A_{Shear\ Wall}$ (m^2)	$\Sigma A_{Masonry\ Wall}$ (m^2)	Shear Wall Density (percent)	Min.Shear Wall Density (percent)
BLD1	0.000	3.725	3.805	0.157	4.550	7.450	7.438	0.313	0.157
BLD2	0.125	0.000	5.188	0.000	4.705	0.000	6.913	0.000	0.000
BLD3	0.300	0.000	4.723	0.000	5.700	0.000	9.600	0.000	0.000
BLD4	0.150	0.000	7.860	0.000	7.290	0.000	11.110	0.000	0.000
BLD5	3.775	0.000	1.190	0.000	2.915	0.000	8.000	0.000	0.000
BLD6	6.060	0.000	4.013	0.000	3.340	0.000	5.860	0.000	0.000
BLD7	0.063	0.000	13.638	0.000	4.293	0.000	8.690	0.000	0.000
BLD8	0.473	0.000	4.485	0.000	5.093	0.000	8.148	0.000	0.000
BLD9	0.000	0.000	7.095	0.000	6.660	0.000	9.675	0.000	0.000
BLD10	1.969	2.719	3.059	0.160	1.750	0.000	6.033	0.000	0.000
BLD11	1.800	0.000	5.290	0.000	1.520	3.966	5.190	0.413	0.000
BLD12	0.000	3.900	3.630	0.167	8.060	1.305	21.000	0.056	0.056
BLD13	0.000	2.125	6.120	0.112	6.925	0.000	12.813	0.000	0.000
BLD14	0.000	0.000	9.085	0.000	6.880	0.000	5.160	0.000	0.000
BLD15	3.649	0.830	5.223	0.032	3.756	0.000	10.743	0.000	0.000
BLD16	0.260	0.000	4.800	0.000	5.300	1.100	9.415	0.044	0.000

Table A.1-2 (continued)

	X DIRECTION				Y DIRECTION				
Building ID	ΣA_{Column} (m^2)	$\Sigma A_{Shear\ Wall}$ (m^2)	$\Sigma A_{Masonry\ Wall}$ (m^2)	Shear Wall Density (percent)	ΣA_{Column} (m^2)	$\Sigma A_{Shear\ Wall}$ (m^2)	$\Sigma A_{Masonry\ Wall}$ (m^2)	Shear Wall Density (percent)	Min.Shear Wall Density (percent)
BLD17	2.493	4.770	5.103	0.170	3.740	4.775	8.030	0.171	0.170
BLD18	0.000	0.000	0.000	0.000	5.775	0.000	7.500	0.000	0.000
BLD19	1.240	4.500	1.875	0.466	1.330	2.778	8.667	0.288	0.288
BLD20	1.970	7.005	5.250	0.337	3.243	0.000	10.300	0.000	0.000
BLD21	2.880	0.000	4.353	0.000	2.325	0.000	9.944	0.000	0.000
BLD22	0.325	0.000	4.205	0.000	7.430	0.000	7.706	0.000	0.000
BLD23	0.000	2.250	2.400	0.174	5.295	4.530	6.870	0.351	0.174
BLD24	0.000	0.000	5.903	0.000	8.600	0.000	11.223	0.000	0.000
BLD25	0.000	0.000	7.752	0.000	3.620	0.000	5.398	0.000	0.000
BLD26	2.608	0.000	7.918	0.000	2.300	0.000	9.846	0.000	0.000
BLD27	0.000	0.000	8.080	0.000	7.750	0.000	11.430	0.000	0.000
BLD28	0.600	3.225	6.810	0.260	2.650	2.650	3.458	0.214	0.214
BLD29	2.790	1.200	4.000	0.154	3.630	1.440	4.000	0.185	0.154
BLD30	2.810	1.100	5.200	0.103	1.530	1.910	5.200	0.179	0.103
BLD31	3.560	4.450	5.200	0.139	5.498	8.919	10.000	0.279	0.139
BLD32	5.940	0.000	5.200	0.000	4.598	7.819	10.200	0.244	0.000
BLD33	2.700	0.000	5.320	0.000	2.700	0.000	9.680	0.000	0.000

A.2 CAPACITY CURVE PARAMETERS OF BUILDINGS

Table A.2-1 Capacity Curve Parameters of Buildings

Building ID		Sd_y (cm)	Sa_y (g)	Sd_u (cm)	Sa_u (g)	C_s	T_e	PF	α	γ	λ	μ
BLD1	X Direction	0.760	0.312	1.393	0.407	0.120	0.313	1.407	0.747	1.946	1.304	1.405
	Y Direction	0.744	0.513	1.383	0.649	0.120	0.242	1.410	0.740	3.163	1.266	1.467
BLD2	X Direction	2.867	0.068	8.158	0.084	0.048	1.301	1.283	0.910	1.293	1.231	2.310
	Y Direction	2.052	0.123	7.781	0.143	0.048	0.821	1.292	0.777	1.985	1.163	3.262
BLD3	X Direction	1.754	0.146	6.940	0.156	0.060	0.696	1.340	0.719	1.745	1.070	3.700
	Y Direction	1.993	0.134	4.702	0.168	0.060	0.775	1.480	0.714	1.590	1.257	1.876
BLD4	X Direction	1.901	0.054	4.615	0.055	0.060	1.193	1.404	0.733	0.657	1.018	2.383
	Y Direction	1.753	0.050	4.579	0.067	0.060	1.193	1.417	0.726	0.601	1.352	1.932
BLD5	X Direction	2.490	0.087	9.502	0.107	0.090	1.074	1.333	0.751	0.725	1.232	3.098
	Y Direction	4.053	0.108	15.600	0.127	0.090	1.226	1.110	0.601	0.725	1.176	3.300
BLD6	X Direction	3.371	0.060	11.409	0.069	0.060	1.509	1.365	0.826	0.820	1.163	2.909
	Y Direction	3.344	0.061	12.830	0.076	0.060	1.486	1.316	0.749	0.761	1.253	3.061
BLD7	X Direction	1.035	0.146	6.506	0.167	0.150	0.534	1.285	0.868	0.845	1.147	5.482
	Y Direction	1.888	0.203	5.171	0.231	0.150	0.611	1.054	0.676	0.916	1.138	2.406

Table A.2-1 (continued)

Building ID		Sd_y (cm)	Sa_y (g)	Sd_u (cm)	Sa_u (g)	C_s	T_e	PF	α	γ	λ	μ
BLD8	X Direction	2.974	0.078	7.742	0.093	0.090	1.239	1.338	0.762	0.660	1.199	2.172
	Y Direction	2.623	0.090	8.890	0.116	0.090	1.085	1.361	0.733	0.730	1.296	2.616
BLD9	X Direction	4.594	0.087	14.163	0.095	0.090	1.461	1.154	0.753	0.724	1.093	2.821
	Y Direction	3.806	0.067	15.352	0.075	0.090	1.507	1.169	0.717	0.537	1.106	3.648
BLD10	X Direction	0.597	0.119	1.641	0.189	0.120	0.449	1.389	0.721	0.716	1.587	1.731
	Y Direction	4.014	0.082	11.981	0.093	0.120	1.407	1.293	0.832	0.566	1.135	2.629
BLD11	X Direction	1.331	0.149	3.570	0.181	0.120	0.600	1.277	0.869	1.077	1.218	2.202
	Y Direction	0.353	0.538	1.191	0.831	0.120	0.162	1.318	0.771	3.458	1.546	2.185
BLD12	X Direction	0.474	0.152	1.345	0.233	0.120	0.354	1.413	0.763	0.966	1.533	1.850
	Y Direction	1.339	0.090	2.276	0.118	0.120	0.774	0.971	0.613	0.459	1.313	1.295
BLD13	X Direction	0.583	0.113	1.709	0.222	0.060	0.455	0.977	0.535	1.012	1.958	1.496
	Y Direction	2.130	0.159	7.664	0.187	0.060	0.734	1.263	0.857	2.274	1.175	3.062
BLD14	X Direction	3.532	0.062	11.286	0.068	0.048	1.516	1.274	0.916	1.180	1.105	2.893
	Y Direction	5.037	0.156	15.201	0.177	0.048	1.140	0.883	0.497	1.613	1.135	2.660

Table A.2-1 (continued)

Building ID		Sd_y (cm)	Sa_y (g)	Sd_u (cm)	Sa_u (g)	C_s	T_e	PF	α	γ	λ	μ
BLD15	X Direction	1.457	0.090	3.111	0.122	0.060	0.805	1.373	0.731	1.101	1.352	1.579
	Y Direction	4.324	0.185	13.407	0.204	0.060	0.970	0.826	0.461	1.420	1.102	2.813
BLD16	X Direction	5.644	0.057	15.528	0.060	0.060	1.995	1.311	0.803	0.764	1.050	2.619
	Y Direction	4.308	0.176	13.565	0.207	0.060	0.993	1.109	0.585	1.715	1.177	2.676
BLD17	X Direction	0.624	0.127	3.003	0.316	0.060	0.445	1.345	0.662	1.400	2.492	1.930
	Y Direction	0.734	0.246	1.660	0.344	0.060	0.346	0.777	0.396	1.623	1.398	1.619
BLD18	X Direction	4.186	0.068	11.499	0.076	0.048	1.576	1.266	0.831	1.174	1.115	2.464
	Y Direction	3.641	0.076	9.470	0.083	0.048	1.391	1.266	0.788	1.242	1.096	2.374
BLD19	X Direction	0.130	0.298	0.535	0.424	0.048	0.132	1.309	0.751	4.668	1.421	2.897
	Y Direction	0.150	0.141	0.688	0.299	0.048	0.207	1.337	0.743	2.178	2.126	2.163
BLD20	X Direction	0.406	0.196	1.467	0.295	0.048	0.289	1.418	0.702	2.861	1.507	2.400
	Y Direction	2.881	0.152	7.173	0.191	0.048	0.873	1.354	0.768	2.432	1.253	1.987
BLD21	X Direction	1.229	0.132	4.183	0.149	0.048	0.612	1.286	0.897	2.470	1.130	3.013
	Y Direction	1.919	0.109	8.965	0.129	0.048	0.843	1.250	0.831	1.882	1.185	3.943

Table A.2-1 (continued)

Building ID		Sd_y (cm)	Sa_y (g)	Sd_u (cm)	Sa_u (g)	C_s	T_e	PF	α	γ	λ	μ
BLD22	X Direction	2.596	0.075	12.686	0.077	0.060	1.180	1.329	0.809	1.011	1.033	4.733
	Y Direction	2.637	0.159	9.630	0.185	0.060	0.816	1.251	0.723	1.922	1.159	3.150
BLD23	X Direction	0.434	0.276	0.890	0.403	0.120	0.252	1.381	0.787	1.811	1.461	1.403
	Y Direction	0.306	0.309	0.737	0.454	0.120	0.200	1.371	0.791	2.037	1.468	1.638
BLD24	X Direction	2.153	0.078	8.664	0.089	0.060	1.055	1.338	0.896	1.163	1.137	3.538
	Y Direction	2.671	0.145	6.835	0.183	0.060	0.862	1.078	0.618	1.489	1.266	2.022
BLD25	X Direction	2.372	0.028	6.780	0.032	0.060	1.850	1.307	0.851	0.396	1.149	2.488
	Y Direction	3.117	0.066	8.703	0.088	0.060	1.377	0.924	0.605	0.667	1.334	2.092
BLD26	X Direction	0.973	0.169	4.310	0.196	0.048	0.481	1.272	0.857	3.025	1.160	3.820
	Y Direction	1.708	0.127	11.639	0.149	0.048	0.737	1.259	0.824	2.172	1.179	5.778
BLD27	X Direction	2.946	0.071	11.562	0.081	0.060	1.292	1.314	0.835	0.989	1.142	3.436
	Y Direction	3.815	0.130	10.039	0.149	0.060	1.087	1.245	0.688	1.489	1.150	2.288
BLD28	X Direction	0.630	0.200	1.517	0.259	0.060	0.356	1.015	0.542	1.805	1.294	1.860
	Y Direction	0.788	0.219	1.986	0.301	0.060	0.381	0.876	0.472	1.721	1.375	1.834

A.3 RESULTS OF PRELIMINARY SEISMIC ASSESSMENT PROCEDURES

Table A.3-1 Results of Preliminary Seismic Assessment Procedure Developed by Yakut [3]

	COLUMN AREAS (m^2)				X DIRECTION				Y DIRECTION				
Building ID	Rectangular (X Dir.)	Rectangular (Y Dir.)	Circle	Square	V_c (t)	V_y (t)	V_{code} (t)	BCPI	V_c (t)	V_y (t)	V_{code} (t)	BCPI	Min. BCPI
BLD1		4.550			371.265	237.034	377.227	0.629	742.529	474.068	377.227	1.257	0.629
BLD2		4.580		0.250	170.542	123.380	79.641	1.551	328.165	237.414	79.641	2.984	1.551
BLD3	0.300	5.700			159.545	101.862	98.143	1.039	296.298	189.172	98.143	1.929	1.039
BLD4	0.150	7.290			204.068	130.288	237.727	0.548	374.498	239.099	237.727	1.006	0.548
BLD5	3.775	2.915			292.204	164.636	244.877	0.673	268.191	151.107	244.877	0.618	0.618
BLD6	6.060	3.340			404.904	228.135	292.148	0.782	333.666	187.997	292.148	0.644	0.644
BLD7		4.230	0.126		109.034	78.881	163.437	0.483	213.410	154.394	163.437	0.946	0.483
BLD8		4.620	0.196	0.750	166.046	106.012	240.967	0.440	293.046	187.095	240.967	0.777	0.440
BLD9		6.660			162.896	104.001	272.346	0.382	325.792	208.002	272.346	0.765	0.382
BLD10	1.970	1.750			401.859	256.567	262.174	0.979	158.654	101.292	262.174	0.387	0.387
BLD11	1.100	0.820		1.400	134.150	97.052	156.287	0.621	438.743	317.413	156.287	2.031	0.621
BLD12		8.060			316.689	229.112	390.661	0.587	320.969	232.208	390.661	0.595	0.587
BLD13		6.925			429.145	310.469	175.765	1.767	446.677	323.153	175.765	1.840	1.767
BLD14		6.880			195.082	124.550	94.176	1.324	390.164	249.100	94.176	2.648	1.324
BLD15	3.444	3.551	0.251	0.160	361.655	230.000	220.444	1.047	297.129	189.703	220.444	0.861	0.861
BLD16	0.260	5.300			178.883	100.788	190.285	0.530	435.322	245.273	190.285	1.290	0.530

Table A.3-1 (continued)

	COLUMN AREAS (m^2)				X DIRECTION				Y DIRECTION				
Building ID	Rectangular (X Dir.)	Rectangular (Y Dir.)	Circle	Square	V_c (t)	V_y (t)	V_{code} (t)	BCPI	V_c (t)	V_y (t)	V_{code} (t)	BCPI	Min. BCPI
BLD17	2.334	3.581	0.318		733.434	468.261	230.926	2.028	773.589	493.898	230.926	2.139	2.028
BLD18		5.775			160.000	102.152	149.404	0.684	320.000	204.304	149.404	1.369	0.684
BLD19	1.240	1.330			464.960	336.379	65.537	5.134	328.582	237.716	65.537	3.628	3.628
BLD20	1.970	3.243			604.693	386.066	133.319	2.897	181.200	115.687	133.319	0.869	0.869
BLD21	2.880	2.325			178.500	129.137	67.086	1.927	166.247	120.273	67.086	1.795	1.795
BLD22	0.325	7.430			204.623	115.291	172.413	0.669	384.555	216.669	172.413	1.258	0.669
BLD23		5.295			281.729	203.820	225.246	0.905	565.564	409.163	225.246	1.817	0.905
BLD24		8.600			204.762	130.730	153.868	0.850	409.523	261.460	153.868	1.701	0.850
BLD25		3.620			97.160	62.032	161.629	0.384	194.320	124.064	161.629	0.768	0.384
BLD26	2.608	2.300			207.594	132.539	81.907	1.618	203.328	129.816	81.907	1.585	1.585
BLD27		7.750			221.428	141.371	173.242	0.816	442.857	282.742	173.242	1.632	0.816
BLD28	0.600	2.650			205.071	130.927	108.721	1.205	209.969	134.055	108.721	1.234	1.205
BLD29	2.790	3.630			298.942	216.273	139.726	1.548	366.516	265.160	139.726	1.898	1.548
BLD30	2.810	1.530			242.100	175.150	251.230	0.695	268.791	194.459	251.230	0.773	0.695
BLD31	3.560	5.498			567.057	362.037	571.868	0.634	902.262	576.049	571.868	1.009	0.634
BLD32	5.940	4.598			437.807	279.518	543.128	0.516	1026.008	655.055	543.128	1.209	0.516
BLD33	2.700	2.700			162.353	117.456	187.493	0.630	162.353	117.456	187.493	0.630	0.630

Table A.3-2 Results of Preliminary Seismic Assessment Procedure Developed by Ozcebe et al. [10]

Building ID	MNLSTFI	MNLSI	NRS	SSI	OR	CMC	DI_{IO}	DI_{LS}	CF_{IO}	CF_{LS}
BLD1	7.2653	2.3623	3	1.032	0.000	2.099	-3.8520	-3.3646	-1.2783	0.0441
BLD2	0.0277	1.6623	3	1.278	0.000	1.128	-2.0430	-1.2742	-0.4794	0.4320
BLD3	0.0322	2.0431	3	1.048	0.000	1.642	-1.3938	-1.4745	-1.0000	0.0345
BLD4	0.0323	1.3420	2	1.000	0.000	1.642	-0.6564	-0.8062	-1.0000	0.0345
BLD5	0.0940	1.9938	3	1.000	0.000	1.642	-0.6257	-1.0190	-0.0016	0.8128
BLD6	0.0660	1.4801	3	1.279	0.000	1.642	-0.4195	-0.0053	-0.0016	0.8128
BLD7	0.0349	3.0017	3	0.969	0.000	2.099	-2.3455	-2.5286	-0.8921	0.8039
BLD8	0.0313	1.2955	2	0.929	0.000	1.642	-0.6873	-1.0309	-1.0000	0.0345
BLD9	0.0411	1.3563	2	1.000	0.000	1.642	-0.6609	-0.8110	-1.0000	0.0345
BLD10	0.0358	1.8132	2	1.000	0.000	1.128	-0.7080	-0.8928	-0.6870	0.0237
BLD11	0.0581	2.3288	1	1.000	0.000	1.128	-0.8916	-0.9131	-0.4794	0.4320
BLD12	0.9734	2.9699	3	0.946	0.000	1.642	-2.6674	-2.8298	-0.6978	0.6289
BLD13	0.0836	2.6695	2	1.000	0.000	1.642	-1.6236	-1.6804	-0.6978	0.6289
BLD14	0.0140	1.9523	3	1.269	0.000	1.128	-1.2661	-0.7334	-0.6870	0.0237
BLD15	0.0671	1.8439	1	1.000	0.000	1.642	-0.0347	-0.2071	-1.0000	0.0345
BLD16	0.0190	0.9584	3	1.000	0.000	1.642	-0.4899	-0.8121	-0.0016	0.8128
BLD17	2.7531	2.9245	2	0.897	0.000	1.642	-1.7867	-2.0999	-1.0000	0.0345
BLD18	0.0270	0.8830	2	0.972	0.000	1.128	-0.6198	-0.8135	-0.6870	0.0237
BLD19	6.1912	5.1182	1	1.000	0.000	1.128	-3.2385	-2.9295	-0.4794	0.4320

Table A.3-2 (continued)

Building ID	MNLSTFI	MNLSI	NRS	SSI	OR	CMC	DI_{IO}	DI_{LS}	CF_{IO}	CF_{LS}
BLD20	0.0888	1.8502	2	1.000	0.000	1.128	-0.7296	-0.9126	-0.6870	0.0237
BLD21	0.0952	2.9392	1	1.333	0.000	1.128	-0.8000	0.0562	-0.4794	0.4320
BLD22	0.0285	1.4001	3	1.000	0.000	1.642	-0.5403	-0.8948	-0.0016	0.8128
BLD23	8.2330	3.2984	3	1.000	0.000	1.642	-5.0998	-4.4986	-0.6978	0.6289
BLD24	0.0155	1.5572	3	1.288	0.000	1.642	-1.2144	-0.5984	-1.0000	0.0345
BLD25	0.0139	1.1997	2	1.000	0.000	1.642	-0.6350	-0.7758	-1.0000	0.0345
BLD26	0.0511	1.9687	2	1.000	0.000	1.128	-0.7297	-0.9249	-0.6870	0.0237
BLD27	0.0103	1.3552	2	0.985	0.000	1.642	-0.6579	-0.8512	-1.0000	0.0345
BLD28	4.8024	4.0020	1	1.286	0.000	2.414	-1.7021	-0.8308	-1.4701	0.0507
BLD29	6.5544	5.7308	3	1.000	0.065	1.810	-4.5469	-4.7057	-0.7692	0.6932
BLD30	1.2186	3.7459	1	1.067	0.064	2.099	-1.1499	-1.4121	-0.8921	0.8039
BLD31	2.3783	2.8674	3	1.000	0.027	2.099	-2.1837	-2.4347	-1.2783	0.0441
BLD32	0.1692	1.8789	1	1.000	0.023	1.810	0.0168	-0.3012	-1.1023	0.0380
BLD33	0.0566	1.9238	3	1.000	0.000	1.642	-2.2218	-2.2371	-0.6978	0.6289

A.4 GLOBAL DRIFT RATIO VALUES

Table A.4-1 Global Drift Ratio Values

	X DIRECTION			Y DIRECTION		
Building ID	Lateral Def. (m)	Height (m)	Global Drift Ratio	Lateral Def. (m)	Height (m)	Global Drift Ratio
BLD1	0.056	12.50	0.004	0.030	12.50	0.002
BLD2	0.190	11.70	0.016	0.114	11.70	0.010
BLD3	0.137	12.80	0.011	0.157	12.80	0.012
BLD4	0.224	13.60	0.016	0.224	13.60	0.016
BLD5	0.296	15.50	0.019	0.320	15.50	0.021
BLD6	0.308	17.95	0.017	0.302	17.95	0.017
BLD7	0.253	10.00	0.025	0.308	10.00	0.031
BLD8	0.313	13.65	0.023	0.288	13.65	0.021
BLD9	0.381	14.10	0.027	0.395	14.10	0.028
BLD10	0.089	13.40	0.007	0.217	13.40	0.016
BLD11	0.086	8.40	0.010	0.014	8.40	0.002
BLD12	0.095	10.75	0.009	0.143	10.75	0.013
BLD13	0.276	10.35	0.027	0.131	10.35	0.013
BLD14	0.237	14.30	0.017	0.172	14.30	0.012
BLD15	0.151	13.30	0.011	0.175	13.30	0.013
BLD16	0.431	17.25	0.025	0.193	17.25	0.011

Table A.4-1 (continued)

	X DIRECTION			Y DIRECTION		
Building ID	Lateral Def. (m)	Height (m)	Global Drift Ratio	Lateral Def. (m)	Height (m)	Global Drift Ratio
BLD17	0.136	13.25	0.010	0.099	13.25	0.007
BLD18	0.249	14.10	0.018	0.214	14.10	0.015
BLD19	0.020	9.10	0.002	0.097	9.10	0.011
BLD20	0.073	12.00	0.006	0.126	12.00	0.010
BLD21	0.088	10.00	0.009	0.118	10.00	0.012
BLD22	0.229	17.00	0.013	0.154	17.00	0.009
BLD23	0.046	9.45	0.005	0.032	9.45	0.003
BLD24	0.196	12.65	0.015	0.167	12.65	0.013
BLD25	0.379	13.40	0.028	0.266	13.40	0.020
BLD26	0.074	11.60	0.006	0.110	11.60	0.009
BLD27	0.246	13.55	0.018	0.208	13.55	0.015
BLD28	0.112	13.40	0.008	0.122	13.40	0.009
BLD29	0.268	10.20	0.026	0.120	10.20	0.012
BLD30	0.542	9.20	0.059	0.491	9.20	0.053
BLD31	0.205	13.60	0.015	0.173	13.60	0.013
BLD32	0.349	13.20	0.026	0.333	13.20	0.025
BLD33	0.146	10.81	0.014	0.142	10.81	0.013